EMBRY-RIDDLE
Aeronautical University™
SCHOLARLY COMMONS

Dissertations and Theses

5-2013

Investigation of a Lagrangian-point Propellant Depot Rendezvous Approach for an Interplanetary Mission to Mars

Joshua W. Ehrlich
Embry-Riddle Aeronautical University - Daytona Beach

Follow this and additional works at: https://commons.erau.edu/edt

Part of the Astrophysics and Astronomy Commons, and the Space Vehicles Commons

INVESTIGATION OF A LAGRANGIAN-POINT PROPELLANT DEPOT
RENDEZVOUS APPROACH FOR AN INTERPLANETARY MISSION TO MARS

by

Joshua W. Ehrlich

A Thesis Submitted to the College of Engineering Department of Mechanical

Engineering in Partial Fulfillment of the Requirements for the degree

of

MASTER OF SCIENCE

in

Mechanical Engineering

Embry-Riddle Aeronautical University
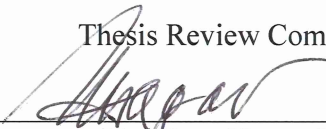Daytona Beach, Florida
May 2013

INVESTIGATION OF A LAGRANGIAN-POINT PROPELLANT DEPOT RENDEZVOUS APPROACH FOR AN INTERPLANETARY MISSION TO MARS
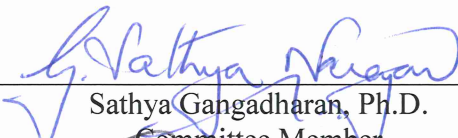
by

Joshua W. Ehrlich

This thesis was prepared under the direction of the candidate's Thesis Committee Chair, Dr. Hamilton Hagar, Professor, Daytona Beach Campus, and Thesis Committee Members Dr. Sathya Gangadharan, Professor, Daytona Beach Campus, Dr. Bogdan Udrea, Professor, Daytona Beach Campus, and has been approved by the Thesis Committee. It was submitted to the Department of Mechanical Engineering in partial fulfillment of the requirements for the degree of Master of Science in Mechanical Engineering.

Thesis Review Committee:
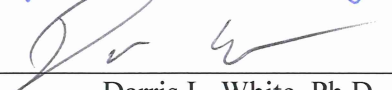
_____
Hamilton Hagar, Ph.D.
Committee Chair

_____
Sathya Gangadharan, Ph.D.
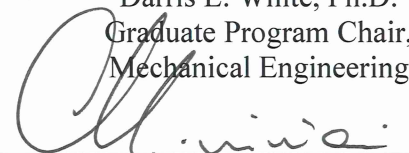Committee Member

_____
Bogdan Udrea, Ph.D.
Committee Member

_____
Darris L. White, Ph.D.
Graduate Program Chair,
Mechanical Engineering

_____
Charles F. Reinholtz, Ph.D.
Department Chair,
Mechanical Engineering

_____
Maj Mirmirani, Ph.D.
Dean, College of Engineering

_____
Robert Oxley, Ph.D.
Associate Vice President for Academics

4-25-13
_____
Date

Dedication

I am dedicating this paper to the two most important people in my life…

My mother, Barbara, raised me as a single parent for most of my entire life. Through the countless career paths she has followed, not once has she ever given up. She has taught me that perseverance, dedication, and love are the lights that can illuminate the darkest of days that fear of impending failure and ongoing uncertainty can be cast away by drive and determination, where selflessness is an over-achieving goal that no one can ever replicate nor demand. She has given me so much in my life, I will always be in her debt. Thank you for all that you have done. You are my mother, I am your son now and forever, I love you.

My grandmother, Pearl, has been the rock of my life. She has given me the love of a mother and the kindness of a friend. From the day I stepped foot on your doorstep to the day I leave to begin my life as a young engineer, you have always been there. You have taught me to never give up, to follow my dreams, and to give everything you got without neither regret nor blame. But most importantly you have shown me that one's heart is a jack of all trades: a tool for compassion and love, as well an emblem of ambition and passion. You are my best friend and you don't understand how much you have meant to me.

Thank you two very much, I love you both with all my heart.

Acknowledgements

I would like to thank Dr. Hamilton Hagar for his continuous support and essential assistance with the completion of this paper. His determination and dedication inspires many students like me to look beyond the text and to dig deeper, to provide the answers to the questions that have yet to be devised, and to push the boundaries to discover one's true potential.

Abstract

Researcher: Joshua W Ehrlich

Title: INVESTIGATION OF A LAGRANGIAN-POINT PROPELLANT
               DEPOT RENDEZVOUS APPROACH FOR AN INTERPLANETARY
               MISSION TO MARS

Institution: Embry-Riddle Aeronautical University

Degree: Master of Science in Mechanical Engineering

Year: 2013

This thesis investigates the feasibility of a refueling station for a beyond Earth orbit (BEO) mission. The propellant depot is located at the L_2-Lagrangian point within the Earth-Moon system. This investigation determines if a refueling mission will reduce propulsive energy requirements necessary for Earth departure of a BEO-vehicle to achieve an interplanetary transfer to Mars. Furthermore, this research presents a trade study which identifies approximate total Δv requirements for a direct and rendezvous mission to Mars as well as the necessary fuel masses to complete each approach. This analysis provides conclusive information in determining the benefits in utilizing a rendezvous location for refueling a spacecraft en versus loading the required fuel masses into a launch vehicle to support a direct transfer to Mars.

Table of Contents

List of Tables

List of Figures

List of Acronyms

ACES   Advanced Common Evolved Stage

AU   Astronomical Unit

BEO   Beyond Earth Orbit

CBC   Common Booster Core

COTS   Commercial Orbital Transportation Services

CRS   Commercial Resupply Services

CR3BP   Circular Restricted 3-Body Problem

DCSS   Delta Cryogenic Second Stage

DEC   Dual Engine Centaur

DRA   Design Reference Architecture

EDL   Entry, Descent, and Landing

ESA   European Space Agency

ESD   Exploration Systems Development

EDUS   Earth Departure Upper Stage

EPF   Extended Payload Fairing

E2L2   Earth-to-L_2 Phase

E2M   Earth-to-Mars Phase

GTO   Geostationary Transfer Orbit

ISS   International Space Station

JAXA   Japan Exploration Agency

LCROSS   Lunar CRater Observation and Sensing Satellite

LEO	Low Earth Orbit
LH2	Liquid Hydrogen
LMO	Low Martian Orbit
LOX	Liquid Oxygen
LPF	Large Payload Fairing
LRO	Lunar Reconnaissance Orbiter
L22M	L_2-to-Mars Phase
NASA	National Aeronautics and Space Administration
NTR	Nuclear Thermal Rocket
RCS	Reaction Control System
RP-1	Refined Petroleum-1
PLF	Payload Fairing
SEC	Single Engine Centaur
SLS	Space Launch System
SOI	Sphere of Influence
SpaceX	Space Exploration Technologies Corporation
TPS	Thermal Protection System
ULA	United Launch Alliance
XEPF	Extra Extended Payload Fairing
ZBO	Zero Boil-Off

List of Terms

avg_E	Average Distance of Earth from the Sun
avg_M	Average Distance of Mars from the Sun
avg_{moon}	Average Distance of the Moon from Earth
avg_{planet}	Average Distance of the Secondary Body Relative to the Sun
$c_{P/L}$	Exhaust Velocity of the Mission Payload
C_j	Jacobi's Constant
$c_{vehicle}$	Exhaust Velocity Based on Vehicle Propulsion Design
e	Eccentricity
ϵ	Structural Ratio Value
$\varepsilon_{phase_{E2M}}$	Specific Orbital Energy of the Earth-to-Mars Approach
$\varepsilon_{phase_{E2L2}}$	Specific Orbital Energy of the Earth-to-L_2 Approach
G	Standard Gravitational Parameter
g_0	Earth Gravitational Acceleration Constant
h_{body}	Parking Orbit Altitude about the Primary Body
$Isp_{vehicle}$	Specific Impulse Parameter per Vehicle Propulsion Design
$L_{\#}$	L# Lagrange Point
$m_{0_{phase_{E2M}}}$	Gross Vehicle Mass per Mission Phase of the Earth-to-Mars Approach
$m_{0_{phase_{E2L2}}}$	Gross Vehicle Mass per Mission Phase of the Earth-to-L_2 Approach

$m_{0\,phase_{L22M}}$	Gross Vehicle Mass per Mission Phase of the L_2-to-Mars Approach
m_{body}	Mass of a Specific Body
$m_{e\,phase_{E2M}}$	Empty Vehicle Mass per Mission Phase of the Earth-to-Mars Approach
$m_{e\,phase_{E2L2}}$	Empty Vehicle Mass per Mission Phase of the Earth-to-L_2 Approach
$m_{e\,phase_{L22M}}$	Empty Vehicle Mass per Mission Phase of the L_2-to-Mars Approach
$m_{f\,phase_{approach}}$	Final Vehicle Mass per Mission Phase of Each Approach
$m_{P\,phase_{E2M}}$	Vehicle Propellant Mass per Mission Phase of the Earth-to-Mars Approach
$m_{P\,phase_{E2L2}}$	Vehicle Propellant Mass per Mission Phase of the Earth-to-L_2 Approach
$m_{P\,phase_{L22M}}$	Vehicle Propellant Mass per Mission Phase of the L_2-to-Mars Approach
$m_{P/L}$	Mass of Mission Payload
μ_{body}	Gravitational Parameter for a Specific Body
Ω	Inertial Angular Velocity
r_{body}	Radius of a Specific Body
$r_{SOI_{2ndBody}}$	Sphere of Influence Radius of the Secondary Body
φ_{fpa}	Flight-Path Angle
$v_{body/E}$	Orbital Velocity Relative to Earth
$v_{body/S}$	Orbital Velocity Relative to the Sun

$v_{esc_{phase_{E2M}}}$	Escape Velocity per Mission Phase within the Earth-to-Mars Approach
$v_{inject_{phase_{E2M}}}$	Velocity to Inject on Transfer Trajectory at Arrival/Departure within the Earth-to-Mars Approach
$v_{inject_{phase_{L22M}}}$	Velocity to Inject on Transfer Trajectory at Arrival/Departure within the L_2-to-Mars Approach
v_j	Scalar Velocity of the Spacecraft for Jacobi's Constant
$v_{\infty_{phase_{E2M}}}$	Hyperbolic Excess Velocity at Arrival/Departure within the Earth-to-Mars Approach
$v_{\infty_{phase_{L22M}}}$	Hyperbolic Excess Velocity at Arrival/Departure within the L_2-to-Mars Approach
Δv_{drag}	Supplemental Velocity Requirement due to Drag at Launch
Δv_{land}	Delta-Velocity for Mars Landing Phase
$\Delta v_{phase_{E2M}}$	Delta-Velocity of a Specific Phase within the Earth-to-Mars Approach
$\Delta v_{phase_{E2L2}}$	Delta-Velocity of a Specific Phase within the Earth-to-L_2 Phase
$\Delta v_{phase_{L22M}}$	Delta-Velocity of a Specific Phase within the L_2-to-Mars Phase
$\Delta v_{total_{E2M}}$	Total Delta-Velocity for the Earth-to-Mars Approach
$\Delta v_{total_{L2rendezvous}}$	Total Delta-Velocity for the Rendezvous Approach
$x_{a_{phase_{E2M}}}$	Apoapsis; Most Extreme Point of the Ellipse per Phase for the Earth-to-Mars Approach

$x_{a_{phase_{E2L2}}}$	Apoapsis; Most Extreme Point of the Ellipse per Phase for the Earth-to-L_2 Approach
$x_{a_{phase_{L22M}}}$	Apoapsis; Most Extreme Point of the Ellipse per Phase for the L_2-to-Mars Approach
x_{L2}	Radial Distance of the Propellant Depot Relative to the Mass Center of the Moon
$x_{p_{phase_{E2M}}}$	Periapsis; Least Extreme Point of the Ellipse per Phase of the Earth-to-Mars Approach
$x_{p_{phase_{E2L2}}}$	Periapsis; Least Extreme Point of the Ellipse per Phase of the Earth-to-L_2 Approach
$x_{p_{phase_{L22M}}}$	Periapsis; Least Extreme Point of the Ellipse per Phase of the L_2-to-Mars Approach

Chapter I

Thesis Overview

Introduction

      Spaceflight has contributed to some of mankind's greatest discoveries, bringing together the most talented and diverse minds to solve some of man's most challenging problems and deepest mysteries. The capability for humans to access the outer reaches of Earth's atmosphere and beyond has proven beneficial for a variety of purposes across different spectrums of society. These benefits have proven vital for pivotal advancements in fields such as biology, communications, navigation, medicine, psychology, physiology, as well as our national and global security to name just a few. These breakthroughs, which span various disciplines of scientific research and study, not only have a significant impact on the people of today, but also lay the foundation for an astronomical "stepping stone" to be used by future generations.

      Man's reach has extended to distances far beyond his own solar system, providing invaluable data for the scientific community and the general public. His curiosity has led him to design journeys never before fathomed. This process has required the most intricate machinery and unique technology ever created. For example, the Voyager 1 spacecraft, launched in 1977, has traveled approximately one hundred twenty-two astronomical units (AU) into space where it is still receiving commands and transmitting data after operating for 35 years [1,2]. Where "one small step for man" echoed across the globe following mankind's first walk on the moon, the next "leap," now within our grasp, stretches to destinations once deemed impossible to reach, going beyond science's

wildest dreams. However, in over forty years, manned exploration has gone no farther than the surface of the moon.

The global fascination in aircraft and spacecraft technology has diminished since the time of early day space exploration. The importance of man's presence in space has often been met with opposing points of view and the impact left on the general public has repelled one another with conflicting force. The significance and relevance of these programs are continuously losing strength in the fight to maintain momentum in many first world nations.

Many advocates, within the government, the scientific community, and the general public, have firmly supported the purposes of space exploration. The post-Apollo period's "next logical step" for the American space program, presented by these advocates, was set in the direction of human exploration of Mars. Since 1975, three-crewed Mars exploration missions have been discussed; however, missions incorporating a satellite or robotic lander have led in all efforts for extending mankind's touch to the red planet [3].

The National Aeronautics and Space Administration (NASA) engineers are seeking new ways to reach destinations beyond our own solar system. President Barack Obama has proposed that humans be sent to orbit Mars and return safely back to Earth by the mid-2030s. NASA is currently developing a multi-stage heavy lift launch vehicle capable of traveling beyond low Earth orbit (LEO). Space Launch System (SLS) will be the most powerful rocket ever created, providing astronauts the ability to reach destinations such as asteroids, Lagrange points, the Moon and Mars [4].

Ultimately, the SLS is planned to serve multiple purposes, specifically to serve as the primary launch vehicle for beyond Earth orbit (BEO) missions. In order to serve SLS and other deep space spacecraft, NASA is developing several technologies to support human exploration of the solar system, one being refueling depots in orbit [5]. These propellant depots would become the "gateway spacecraft" for future exploratory missions to the Moon and would lay the groundwork for more ambitious trips to Mars' moons and even Mars itself [6]. By including these "pit-stops" into BEO mission design, engineers and scientists can possess a key advantage in designing optimal interplanetary trajectories for deep space vehicles.

Statement of the Problem

The current cost for access to space is in the area of thousands-of-dollars per pound of payload. The larger, non-man-rated systems with low labor costs occupy the lower portion of this area while those man-rated systems with intricate payload systems are responsible for the higher values. There have been a plethora of systems designed to gain access to space including various classes and types of rockets, propulsion systems, staging, reusability options, take-off and landing options, and material and controls options. Programs all across the globe have designed and tested countless combinations of these different subsystems; however, an ideal solution which incorporates maximum benefits with minimum drawbacks for manned deep space exploration of these different options has never been accomplished [7].

From the Apollo Moon landings to deep space satellite launches, NASA has utilized Hohmann transfers and planetary flybys for injecting spacecraft for both local

locations and distant destinations. These missions, however, are extremely costly in terms of price and fuel [8]. For example, the heavy-lift man-rated rockets such as the Saturn V and space shuttle required large masses of fuel for powering the engines that provided the sufficient amount of thrust to lift their enormous structures to orbit. The Saturn V rocket (which ran from 1964 to its decommissioning in 1973) required 8.7 million pounds of thrust to lift a gross average mass of 6 million pounds [9]. The three-stage rocket had separate fuel requirements per stage – the first stage used a combination of RP-1 (Refined Petroleum-1) and liquid oxygen, the second and third stages used a combination of liquid oxygen and liquid hydrogen. The Saturn V rocket required 947,459 gallons (7,907,000 pounds) of fuel and oxidizer with an average cost of $185 million (due to inflation, in 2013 dollars that is equivalent to $1.17 billion). Overall, the Saturn V allocated $6.5 billion in total costs (equivalent to $46.56 billion in 2013 dollars) [10, 11].

The space shuttle, one of the most iconic images of NASA's manned spaceflight program, was commissioned in 1981 and was flown until the program's retirement in 2011. The program's five orbiters flew a total of 135 missions, delivering several notable payloads such as the Hubble space telescope, Galileo spacecraft, Magellan spacecraft, and numerous ISS (International Space Station) components. The gross liftoff weight for the space shuttle was approximately 4.5 million pounds and required 7.8 million pounds of thrust to lift the external fuel tank, two solid rocket boosters, payload(s), orbiter and crew to LEO [12-14]. Both the orbiter and external fuel tank carried 835,958 gallons (6,976,000 pounds) of its principal propellants – liquid hydrogen, liquid oxygen, hydrazine, monomethylhydrazine, and nitrogen tetroxide – the total cost (in 2001 dollars) was $1,380,000 [15]. Additional costs for fuel had the potential to be doubled or tripled as

launch scrubs would require all fuel to be depleted and then be replenished fully for the next launch attempt. Over the life of the program the average cost per launch was about $1.2 billion [16].

Cost is the biggest driver to designing and constructing a system of such magnitude such as a spacecraft, which encompasses a wide array of one-of-kind technologies within its design as well as a strategic mission design. Too often, however, this practice of minimizing impacts to costs of an overall mission is performed late in the design process with minimal influence on the designs [17]. With NASA's budget seemingly static or shrinking annually, engineers today are seeking to adopt ways to design spacecraft and its mission with the intention of being affordable, to support design, development and maintenance, as well as serve multiple purposes.

Access to space is a high-dollar necessity. Current technology constraints for traveling to further destinations than previously explored prevent manned spaceflight the opportunity to conduct deep space exploration. However, the associated costs to development of a new vehicle to deliver payloads are a significant amount. Thus, engineers must make use with the technology available in order to minimize impacts to the dollar amount connected with the project. Savings to costs, without any manipulation or alteration to the design of current launch delivery vehicles, can be practiced with the necessary fuel masses associated with these deep space missions. Travel to Mars poses many challenges and limitations surrounding mission and vehicle design. Consideration for estimated fuel consumption must be taken into account when designing such a vehicle. Designs must include the determination of the vehicle masses based on the required fuel mass to support the mission. A prime mission design will require marginal

propellant energy requirements, minimal propellant masses, and a vehicle design that incorporates minimal impacts to the overall mass of the spacecraft and costs of the mission.

Scope

      The human space exploration initiative has not been tested in the last forty years. Our technological advances continue to grow but our reach "to infinity and beyond" has dwindled over the last several decades. Implementing future technologies to address multi-mission objectives are becoming increasingly sought after. By designing the future of space exploration with the requirements of economic feasibility and performance efficiency, the opportunity to move forward in expanding our presence in our solar system and beyond is an achievable objective.

      The scope of this paper looks to determine practical and technical advantages of implementing a rendezvous scenario at a Lagrange-point propellant station within the Earth-Moon system en route to Mars. With the use of patched-conic approximation, a comparative analysis is constructed to relate the propellant and fuel mass requirements associated with two basic mission profiles en route to Mars, a direct approach and rendezvous approach at a Lagrange point propellant depot. Although this study is conducted using basic, preliminary calculations, an error analysis (provided later in Chapter IV) explains that the minimal errors associated with this approach versus one of greater detail does not affect the objectives under investigation in this study.

      This analysis explores two basic mission profiles, which utilize 1) coplanar Hohmann transfers to represent the minimal impulse energy required for each transfer, 2)

planetary circular orbits, and 3) impulsive velocity maneuvers per phase within each profile. This investigation does not take into account the necessary costs associated with supporting the Lagrange point propellant depot. It is assumed within this paper, prior to execution of the mission under study, that sufficient motivation and commitment to support the propellant depot were already put in place to build the necessary infrastructure on the moon to supply fuel to the propellant depot.

This study serves to identify which of the two scenarios is more economical and efficient in terms of costs and design for delivering a chosen spacecraft to a pre-determined low Martian orbit (LMO). It is assumed within this investigation that the necessary propulsive energy requirements within the rendezvous approach are solely associated with the necessary maneuvers to rendezvous and depart the propellant depot. All other phases, including departure from Earth, arrival at Mars, and landing on the Martian surface, are all identical within both mission profiles under investigation. This approach is reasonable for a valid comparison of the two mission designs.

Mars-Direct Approach

In the past, traditional methods of transporting manned spacecraft beyond LEO have been confined within cis-lunar space (within the Earth's sphere of influence (SOI)). A voyage reaching to further destination, however, requires substantial infrastructures to support the greater fuel requirement, life support systems, etc. A voyage to Mars, for example, requires a substantial amount of propellant and vehicle mass to support the crew and deliver the mission payload. These large masses are beyond the capabilities of what current launch delivery vehicles available can accommodate in a single launch.

The direct approach is one which involves single (or staged) departure and arrival impulses. The size of such a vehicle to support a mission to Mars requires the use of multiple launch vehicles. Integration of these vehicles could be carried out at LEO; however, the assembly process would be highly complex and might require the process be carried out in multiple missions. Numerous launches must be initiated in order to deploy the pre-determined quantity of vehicles needed to supply fuel for the direct trajectory to Mars. Proper fuel systems to power those vehicles in LEO waiting to be assembled require both power to provide cooling for fuel and propulsive controls to keep the vehicle in a safe orbit. This approach carries a significant price tag in providing the technology necessary to support a direct approach to the red planet.

L_2-Lagrange Point Propellant Depot Rendezvous Approach

An alternative to the direct approach which is presented in this paper is the utilization of an intermediation refueling depot prior to departure from the Earth-Moon system. This fuel source, located at the L_2-Lagrange point of the Earth-Moon system, provides the necessary propellant to power a vehicle to transfer from that location to LMO. Fuel is provided to the depot by way of transfer from stations located on the surface of the Moon, where it is assumed to be manufactured. The propellant depot at the L_2-Lagrange point provides the facility for a spacecraft to rendezvous, dock, and refuel. As shown later, although the necessary gross propulsive energy requirements required for the rendezvous approach at the propellant depot is somewhat larger than transfer a spacecraft directly to the planet, the necessary fuel and propulsive system support masses associated with the refueling mission en route to Mars is less.

The assumption within this paper is that there is in place on the surface of the Moon the necessary infrastructure to provide fuel to the propellant depot. This fueling capability is only considered advantageous for refueling missions visiting the propellant depot when it is located at the L_2-Lagrange point. Although the distance from Earth to the stable Lagrange points, L_4 and L_5, are the same in comparison to the distance to the unstable L_2-Lagrange point, the ease for transporting fuel to be stored in the propellant depot at L_2 is much greater due to the distance the L_2-Lagrange point is located from the mass center of the Moon. Comparing that distance to the distance the fuel must be transported to reach a propellant depot at L_4 or L_5, the advantage lies in the placement of the propellant depot at the L_2 point of the Earth-Moon system.

Significance of the Study

Although our ability to travel to destinations beyond our atmosphere has been proven possible, the ability to maintain that capability has been static for several decades. As the next chapter in human exploration is being written, a strategy must be devised in order to expand mankind's boundaries beyond that of which has already been explored. A Lagrangian fuel depot would provide an advantageous location towards interplanetary exploration by providing cryogenic fuel storage and transfer capabilities for multi-purpose functionality. This station shall be a benefactor in providing a valuable position in Earth-neighborhood campaigns and BEO missions. In addition to propellant supply, these depots may serve as servicing platforms where propellant is stored and transferred to reusable vehicles as needed. They will also provide hubs for vehicle maintenance and upgrades, as well as provide transfer locations for crew logistics and payloads.

Constructing a depot in the vicinity of the L_2 region facilitates round-trip exploration by initiating and designating this location as a relay point, thus leading to a reusable transportation system. Adoption of this mission design theory enables large, beyond-LEO missions to be conducted without super heavy lift vehicles required to lift the large masses of fuel necessary for long-duration flights [13, 18]. While the necessity for space accessibility and operations continue to move forward, the development of in-space refueling is essential [12].

<center>**Chapter II**</center>

<center>**Review of the Relevant Literature**</center>

Introduction

To accomplish the objectives as stated in Chapter 1, a review of literature relevant to this project was performed. The purpose of this paper is to determine whether a propellant depot at the L_2-Lagrange point of the Earth-Moon system is both plausible and economical in terms of fuel costs and mass requirements for the propulsion system necessary to support the necessary propellant mass. A comparative analysis is conducted between the exploitation of this intermission rendezvous location with that of a direct transfer to Mars. Information, data and analysis from the scientific community are incorporated into this paper in order to rationalize, establish, and provide support for the objectives.

History and Development of Interest

Why Mars?

For thousands of years, humans in many ancient civilizations have been drawn to Earth's neighboring celestial body, Mars. These early ancestors gave many names to this heavenly body: the Egyptians called it Har decher (the Red One), the Babylonians named it Negral (the Star of Death), the Greeks designated it Ares and the Romans called it Mars (each representing the God of War). Early philosophers and astronomers studied the planet's "wandering" motion, which was once believed to follow a geocentric frame of reference. This belief lasted for hundreds of years until many philosophers, mathematicians, and astronomers observed and analyzed the body in greater detail.

<center>11</center>

Aristarchus, followed by Copernicus and later confirmed by Brahe and Kepler, disputed the belief that Mars followed an orbit similar to our own planet. It was later proved that in fact, all the planets revolved around the Sun [19].

Further study of Mars would stretch over the next several hundred years since its heliocentric life cycle was established. In 1783, William Herschel, who years earlier discovered the planet Uranus, found that Mars was tilted at an angle of almost 24 degrees. This finding led to the belief that Mars, like Earth, Mars was similar to our own seasonal calendar. However, due to the Martian year being almost double to that of Earth's, seasons on the red planet were twice as long [19].

In 1877, Asaph Hall, director of the U.S. Naval Observatory, discovered Mars' two moons, Phobos and Deimos (from the Greek translation meaning *fear* and *flight*, respectively). Data collected from his observations led to Hall's estimated calculation of Mars' mass as being 0.1704 times that of Earth, which is accurate to within 2×10^{-4} decimals less than the currently accepted value. That same year, an Italian Virginio Schiaparelli, spent the summer observing the geologic features of the Martian surface. As director of the Milan Observatory, Schiaparelli observed for the first time a large system of winding lines and markings. He called these lines *canali*, which means "channels", "grooves", or "canals" in Italian. His discoveries startled the human imagination on a grand scale [19].

Twenty years later, an American amateur astronomer and mathematician, Percival Lowell, dedicated himself to finishing Schiaparelli's earlier work. During the summer and fall of 1894, Lowell observed the surface of Mars day and night, constructing maps of the planet's geographic features. Upon completion of his illustrated parchment,

Lowell's maps displayed 184 canals, twice as many as Schiaparelli initially claimed. His discoveries led to his announcement to the world that the canals were constructed by intelligent beings. Powell's eye-raising pronouncements, most astronomers were not convinced and disputed his statements. As Powell's theories slowly eroded over time, the effect it left on the general public regarding extraterrestrial Martian life led to widespread interest in Mars [19].

Lagrange's Influence

The first three collinear Lagrange points (L_1, L_2, and L_3) were discovered by Leonhard Euler in 1772 [8]. A few years later, an Italian-born French astronomer and mathematician, Joseph Louis Lagrange, was working on a trajectory formulation when he came across his renowned discovery [20]. Lagrange was able to demonstrate a constant pattern within a three body system, both confirming Euler's collinear locations (L_1, L_2, and L_3) as well discovering two additional equilateral points (L_4 and L_5) with conic section orbits. Historians have inaccurately credited Lagrange for naming all five of these libration points, since it was Euler who discovered the first three points several years before him [8]. However, common literature addresses all five locations as Lagrange points, thus this paper will address them by that affiliation.

Within the last 40 years, attention and study of the Lagrange points was sparked by Gerald K. O'Neill, a NASA scientist-astronaut candidate, and one of the first promoters of space colonization. Published in September 1974 in the journal *Physics Today*, O'Neill wrote a paper titled "The Colonization of Space" in which he spoke about the enormous potential and advantage human space colonization presented. O'Neill

envisioned his proposed colonies to be located at the L_4 and L_5 Lagrange points, and went as far as to say that human space colonization would solve at least five of the most serious problems now facing the world (raising the standard of living for every human being; protecting the biosphere from damage caused by transportation and industrial pollution; finding high quality living space for a human population doubling every 35 years; finding clean, practical energy sources; preventing heat overload on planet Earth) [21]. O'Neill's knowledge and passion ignited an instantaneous rise across the United States, eventually attracting pro-space followers and enthusiasts, which included engineers and scientists who not only supported his viewpoint and work but also began to study the potential and plausibility that an object, let alone a space colony, could be placed at any of the Lagrange point locations [22].

Moving forward to 2009 the White House Office of Science and Technology requested NASA to initiate an independent review of the ongoing U.S. human spaceflight programs. Working in conjunction with the U.S. Human Space Flight Plans Committee, NASA formed an Engineering Analysis team, comprised of representatives from all the NASA centers, to address the various areas of interest for human exploration in order to devise a practical proposal for future exploration scenarios.

Five exploration strategies were created. The one of greatest interest was the flexible path scenario. The purpose of this scenario was to study a wide range of inner solar destinations. This scenario was not to incorporate any such transitory missions to the surface of any locations with deep gravity wells, such as the Moon, Mars, and Venus; however, the scenario did include principal destinations such as the Earth-Moon L_1 and L_2 Lagrange points.

Overview of Analysis

Patched Conic Approximation

Walter Hohmann proposed a theory which suggested the minimum change in velocity for a transfer between two orbits could be accomplished through the use of two tangential burns (in which case the flight-path angles within this paper are equal to zero) [23]. The proposed theory, known today as the Hohmann transfer, defines an elliptic transfer between two orbits. The geometry of the elliptical Hohmann transfer trajectory is defined by the semi-major axis distance, which spans the co-axial distance on the two-dimensional reference plane, and its eccentricity.

The term "conics" refers to the two-body orbit where the focus is centered at the attracting body [24]. Conics have one of the following shapes: circular, elliptical, parabolic, and hyperbolic. In the method of patched conics, a sequence of trajectories are computed relative to a central body, the one for which the spacecraft is experiencing the greatest gravitational influence. Similar statements can be made for a spacecraft's orbital motion relative to any planetary body. This approach is dependent largely on how close the spacecraft is to the attracting body. When perturbing accelerations of a third body (or more) affect the perturbing influences of the primary body, patched conic approximation can produce error in determination of the spacecraft's orbit.

The method of patched conic approximation is a simplified technique for trajectory calculations in a multiple-body system. The simplification involves dividing space into various parts by assigning each of the observed bodies within the environment of the problem being investigated its own SOI [8]. Trajectories conducted within a body's

SOI are treated as two-body problems with the planet considered as the central attracting body [25].

Due to the fact that interplanetary disturbances are so vast and can span from far reaches of space, the gravitational influence a body may emit is often neglected. For the purpose of this paper, however, spheres of influence are considered when initiating a Hohmann transfer from the planet/body for which the spacecraft is departing or arriving. For the transfer from Earth to Mars, the gravitational influence of Earth is only considered up to a distance where its gravity no longer dominates the Sun. When the spacecraft departs Earth, the Sun's gravity "takes over" as the gravity-inducing body affecting the spacecraft until the trajectory reaches the SOI of Mars, in which the planet's gravitational influence gains precedence over the Sun.

The SOI is determined from the relation between the mass of the central body and the Sun, respectively. When the spacecraft is near the planet, the distance from the spacecraft to the sun is considered to be the same as the distance from the central body to the sun (avg_{planet}) (the order of magnitude in difference between the two distances is minute, thus the average planetary distance to the Sun is used). The product of the mass relation and the average distance from the central body to the Sun is calculated in Equation 1.

$$r_{SOI\,2ndBody} = avg_{planet} \left(\frac{m_{planet}}{m_{Sun}} \right)^{\frac{2}{5}}$$

Equation 1 – To calculate the sphere of influence for a secondary object of lesser mass.

Lagrange Point Implementation

From aircraft and ships to automobiles and spacecraft, fuel efficiency of these propulsion systems designed to accommodate long distance travel has been a constraint for mankind since the 1800s. As early as 1928, scientists began studying the argument that interplanetary travel was only possible by way of pre-positioning propellant stations in orbit to support any large-scale journey beyond Earth. Construction of these facilities has gained increasing support. With the intentions for receiving, storing, and dispensing propellant to visiting spacecraft would serve an important role [14].

Engineers have investigated ways to utilize these points in space, or "gateways" as they have been called. In fact, several spacecraft have already utilized the L_1 and L_2 points of the Earth-Sun system (for example, the Wilkinson Microwave Anisotropy Probe) [13, 26].

With respect to the rotating frame of the Earth-Moon system (for the purpose of this study), the Lagrange points are located relative to the system's barycenter. The circular restricted 3-body problem (CR3BP) arises from this definition. A solution of the CR3BP cannot be obtained in closed form but as an integral of motion, obtained from calculation of Jacobi's constant. The basis for using Jacobi's constant is to provide a basis for the location of the Lagrange points within a system. These points are located within distinct regions of motion about either the primary or secondary masses where an object (of insignificant mass) has zero relative velocity (as well, as the edge of the regions; see Appendix for derivation of the Jacobi integral) [27]. The Lagrange points, located in the *x-y* frame, are considered to be stable locations when small displacements occur parallel to the *z*-axis. Because of the necessary controls to maintain a spacecraft's

17

orientation at the L_1, L_2, and L_3 points, these collinear points are considered to be unstable. The L_4 and L_5 Lagrange points require minimal impulsive maneuvers from a spacecraft intending to maintain its position, thereby defining these two points as stable [28].

An Earth-Moon Lagrange point mission offers an ideal stepping stone to deep-space missions of longer duration serving potential applications such as propellant re-supply or even gateways for Mars exploration [29]. Other applications can include propellant storage, docking platforms/stations, and infrastructure to support science. Location of the Lagrange points in the Earth-Moon two-body is shown in Figure 1.
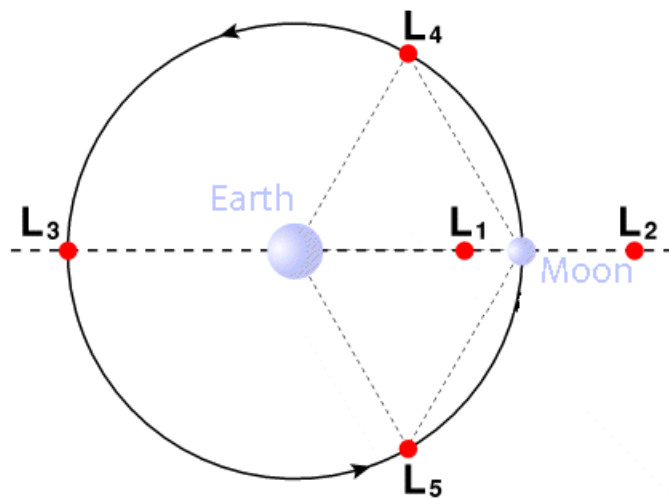
Figure 1 – Illustration representing the Lagrange point orientation within the Earth-Moon system [27].

<center>**Chapter III**</center>

<center>**Methodology**</center>

Mars-Direct Approach

      Spacecraft departure and arrival within the Earth-Mars system uses patched-conic

dynamics, which incorporates both elliptical and hyperbolic trajectories for departure

from Earth and arrival to Mars.

The process for the Mars-Direct mission design is as follows:

1. Spacecraft enters Earth parking orbit following launch

2. Departure on a hyperbolic trajectory from the Earth-Mars periapsis

3. Spacecraft motion transforms to elliptical transfer trajectory at edge of Earth's

    SOI

4. At Mars' SOI, spacecraft motion transforms to a hyperbolic arrival trajectory

5. Injection into Mars' LMO

6. Aerobraking for reduction in spacecraft entry velocity into Mars' atmosphere

7. Mission payload landing

L_2-Lagrange Point Propellant Depot Rendezvous Approach

      In contrast to the Mars-direct approach, the trajectory for spacecraft departure

from Earth and arrival at the Earth-Moon L_2-Lagrange point propellant depot is a

Hohmann trajectory. The use of patched-conL_2ics comes into play from departure at the

rendezvous location and arrival at Mars.

The process for the L_2-Lagrange point propellant depot rendezvous mission design is as follows:

1. Spacecraft enters Earth parking orbit following launch

2. Spacecraft departs Earth-Moon periapsis on a Hohmann transfer

3. Rendezvous at the L_2-Lagrange point propellant depot; spacecraft docks to station.

4. Departure from depot on a hyperbolic trajectory from the Moon-Mars periapsis

5. Spacecraft transforms to elliptical departure trajectory at edge of Earth's SOI

6. Onset to Mars' SOI, spacecraft shifts to a hyperbolic arrival trajectory

7. Injection into Mars' LMO

8. Aerobraking for reduction in spacecraft entry velocity into Mars' atmosphere

9. Mission payload landing

The propulsive energy requirements associated with these maneuvers entail the necessary propellant masses to fuel these dynamics. These calculations for both the Mars-direct and rendezvous approaches are carried in Chapter IV of this thesis.

Chapter IV

Analysis

Mission Objective

For the last several decades, space programs all across the globe have sent unmanned spacecraft to Mars to survey and record numerous scientific data and information. Such missions include atmospheric, chemical, and geologic studies of Mars as well imagery and radiation analyses for a wide array of private and governmental customers. An abundance of these missions, however, have failed to fulfill their mission objectives. Since the 1960's there have been a total of 40 satellite or lander missions to Mars between the American (NASA), Russian (Roscosmos), and Japanese (JAXA) space programs, as well as the European Space Agency (ESA). Of those missions, only 16 have successfully fulfilled their purpose (a 40% success rate), 7 of which have landed on the planet's surface [30].

NASA has conducted or sponsored numerous studies on guiding human exploration missions beyond LEO. In essence, these studies are to understand and determine the necessary requirements for missions to the Moon and Mars, as well as in the context of utilizing these locations for other exploratory missions. The Mars Design Reference Architecture (DRA) 5.0, a mission overview authored by NASA, outlined the system framework for conducting a multiple-site exploration mission to the red planet. The primary objective of this mission would be to understand the global history of Mars, and thus, would require a unique location for each mission [31]. Analyzing and comparing the data and information collected from the different locations, mission design teams

21

would have the opportunity to determine which site would be deemed as possessing the greatest potential for supporting a permanent human colony. Development of a permanent base on Mars would look to accomplish an overall goal of constructing a self-sufficient, autonomous human presence on the planet [32]. Each of the three missions would utilize a "forward deploy" strategy, where the essential habitat and sub-systems assets necessary to support the crew and the mission would be sent to Mars prior to crew arrival. The purpose of this initial deployment would be to allow for verification and checkout of the sub-systems within the habitat to minimize mission risk prior to the crew arrival.

Mission Payload

As stated previously, this thesis analyzes and compares the propulsive energy and mass requirements between two interplanetary missions to Mars. Arrival at the planet, however, would serve a secondary purpose. Upon reaching a pre-determined LMO parking altitude, the payload transfer vehicle would precede in inserting a permanent, self-sustaining habitat through the Martian atmosphere to land safely on the surface.

A self-contained habitat concept, as shown in Figure 2, was selected as the permanent habitat payload to be delivered. This payload design was chosen for several reasons. First, the habitat design allows for the incorporation of a propulsion integration system similar to that of the Apollo program's lunar module, to be utilized for both entry and departure. Second, the habitat is a single modular entity where neither additional construction nor assembly of any secondary structural components will be required of the main structure. A single mission will transfer the payload from LMO where it will be

deployed and injected into the Martian atmosphere for landing on the surface of the planet [33].
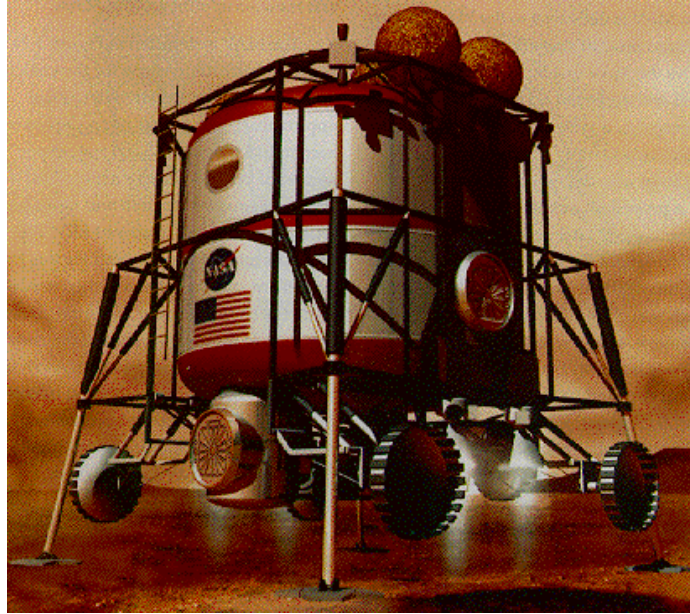
Figure 2 – Artist's illustration depicting a landing of a Mars manned exploration habitat. The mission payload is to be delivered to the Martian surface where it be configured to support crew inhabitation in a future mission [34].

The habitat is fitted to accommodate a total of six astronauts for a total of 500 days on Mars. This crew quantity provides skill versatility for team-affiliated activities as well as singular expertise in various areas provided by each astronaut beneficial to the success of the mission [35]. The mass of the habitat is comprised primarily of structural components and life support systems for the crew. These components include frames for the habitat's pressurized shells, floor systems including floor beams and panels, and secondary life-support systems such as a surface nuclear power source, breathable air systems, and a water production and filtration assembly [33, 35]. The habitat is designed to have autonomous capability for unloading, relocation, and subsystem operations for a significant amount of time without the physical presence of humans required. These life

support systems are necessary for a precursor mission in order to ensure all systems are operable and promote safety, efficiency, and reliability for future crew arrivals to the habitat. The total mass of the habitat is 25,000 kg [33, 36].

Mission Parameters

This section identifies the mission design parameters for each approach as well as assigns the necessary scientific data for each independent variable. Defining initial conditions such as position and velocity provides a consistent plan of action for both scenarios to follow as well as identifies which values for each approach were intentionally varied for the purpose of comparing the two scenarios. These parameters are constructed for the purpose of defining interplanetary reference positions of the bodies along with their planar locations within the Sun, Earth, and Mars frames of reference (Table 1). The gravitational constants for the Sun, Earth, the Moon, and Mars as well as their respective masses are defined in Table 2.

Table 1 – Description of each body's average radial distance and mean distance values relative to their mass center [23]. The radius for each body's SOI is shown. The radial distance values for Earth, the Moon, and Mars are represented by r_E, r_{moon}, and r_M, respectively; their mean distance values as avg_E, avg_{moon}, and avg_M. The mean distance values of Earth and Mars are relative to the mass center of the Sun while the Moon is in reference to the mass center of the Earth.

Geometric Values for the Selected Bodies			
	Radius	**Mean Distance**	**SOI Radii**
Earth	6,378 km	149,598,023 km	925×10^3 km
Moon	1,738 km	384,400 km	66.1×10^3 km
Mars	3,397 km	227,939,186 km	577×10^3 km

Table 2 – Values of the mass and gravitational parameters for the select bodies. The accuracy of the standard gravitational parameter is more accurate than the standard gravitational parameter or mass of the body. The uncertainty pertaining to the accuracy of the standard gravitational parameter for a system of mass-significant bodies (i.e. the heliocentric solar system) is 1 to 500,000,000 compared to the uncertainty per G or M of the entire system to be 1 to 7,000 (each) [37].

Mass Values for the Selected Bodies		
	Standard Gravitational Parameters	**Mass**
Sun	$1.327 \times 10^{11} \dfrac{\text{km}^3}{\text{s}^2}$	1.9891×10^{30} kg
Earth	$3.986 \times 10^{5} \dfrac{\text{km}^3}{\text{s}^2}$	5.9742×10^{24} kg
Moon	$4902.799 \dfrac{\text{km}^3}{\text{s}^2}$	7.3483×10^{22} kg
Mars	$4.305 \times 10^{4} \dfrac{\text{km}^3}{\text{s}^2}$	6.4191×10^{23} kg

The maxima and minima points of the Hohmann transfer known as the periapsis and apoapsis. These locations are designated as the orbital altitudes relative to the Earth and Mars are defined in Equation 2.

$$h_E = 300 \text{ km}$$

$$h_M = 300 \text{ km}$$

Equation 2 – Parking orbit altitude of the spacecraft relative to their referenced body's surface.

These values represent the parking orbits for which the spacecraft is located in LEO and LMO relative to the surface of Earth and Mars, respectively. The radial distance of the propellant depot is determined from the difference between the L_2-Lagrange point location within the Earth-Moon system with the average longitudinal distance the Moon is located at its radial center relative to Earth. This value serves as the rendezvous location at the propellant depot; parking orbit altitude is not considered during docking/undocking operations of the spacecraft at the propellant depot.

It is assumed that the Earth and Mars orbits, along with the spacecraft parking orbits in LEO and LMO, respectively, are circular. Each orbital velocity value is calculated (Equation 3) and arranged in Table 3.

$$v_{body/referenced\ body} = \sqrt{\frac{\mu_{referenced\ body}}{avg_{body}}}$$

Equation 3 – To calculate the orbital velocity of a body relative to a secondary body of greater mass based on its average distance from the larger body.

Table 3 – Within the Sun-centered system are the orbital velocities of Earth and Mars. The relative orbital velocity of the Moon sits within a geocentric frame of reference.

Orbital Velocity of the Planetary Body Relative to the Referenced Body	
	Orbital Velocity
Earth	$29.783\,\dfrac{km}{s}$
Moon	$1.018\,\dfrac{km}{s}$
Mars	$24.128\,\dfrac{km}{s}$

Design Approach per Mission Scenario

The following section compares the two mission profiles in question; a Mars-direct approach and rendezvous refueling approach. These findings illustrate the propulsive energy requirements for each mission. The total Δv values calculated include the velocities necessary to ascend to LEO and descend to the surface of Mars.

Mars-Direct Approach

To conduct a comparative analysis on different mission design profiles and their respective Δv and energy requirements, a control (or baseline) approach is carried out using conic and patched-conic approximation methods. This is conducted in order to determine the advantage for implementing a refueling location at the L_2-Lagrange

26

location within the Earth-Moon system. This investigation finds the fuel and structural

masses required to support a propulsion system designed to transfer a spacecraft directly

transferring to Mars.

The location of the first tangential burn for departure is located at the periapsis of

the Hohmann transfer. The major axis of the transfer is comprised of the sum of the

radius of the Earth circular parking orbit, the mean distance from the Earth to the Sun, the

mean distance from the Sun to Mars, and the radius of the Mars circular parking orbit. A

second tangential burn is initiated for injection in Mars circular parking orbit about Mars

once the spacecraft arrives at the apoapsis location of the Earth-Mars transfer trajectory.

These values are

$$x_{p_{E2M}} = avg_E + r_E + h_E = 149{,}604{,}701 \text{ km}$$

Equation 4 – The distance of periapsis relative to Earth's mass center, relative to the Earth-Mars two-body system.

and

$$x_{a_{E2M}} = avg_M + r_M + h_M = 227{,}942{,}883 \text{ km}$$

Equation 5 – The apoapsis location relative to the Mars mass center within the Earth-Mars two-body system.

The semi-major axis of the Mars direct approach is calculated in Equation 6, which is a

driver to the elliptical eccentricity of the Hohmann transfer geometry.

$$a_{E2M} = \frac{x_{p_{E2M}} + x_{a_{E2M}}}{2} = 188{,}773{,}792 \text{ km}$$

Equation 6 – Average distance to the centroid of the ellipse to conduct a Hohmann transfer from Earth periapsis to Mars apoapsis.

The specific orbital energy for the spacecraft within the heliocentric reference system is

calculated in Equation 7.

$$\varepsilon_{E2M} = -\frac{\mu_S}{2a_{E2M}} = -351.479 \ \frac{\text{km}^2}{\text{s}^2}$$

Equation 7 – The specific orbital energy, including both kinetic and potential energies, to travel on an elliptic trajectory from Earth to Mars.

At Earth parking orbit altitude, the spacecraft orbital velocity is calculated in Equation 8.

$$v_{E\,E2M} = \sqrt{\frac{\mu_E}{r_{p\,E2M}}} = 7.726 \ \frac{\text{km}}{\text{s}}$$

Equation 8 – Orbital velocity of the spacecraft relative to Earth mass center at parking orbit altitude, h_E.

The velocity of the spacecraft at periapsis is found in Equation 9.

$$v_{peri\,E2M} = \sqrt{2\left(\varepsilon_{E2M} + \frac{\mu_E}{avg_E}\right)} = 32.728 \ \frac{\text{km}}{\text{s}}$$

Equation 9 – Calculation for the spacecraft velocity at periapsis within the Earth-Mars system.

Locating the spacecraft at periapsis of the Earth-Mars transfer, relative to the Sun, the escape velocity from Earth is calculated in Equation 10 while the hyperbolic excess velocity necessary to reach Mars is calculated in Equations 11.

$$v_{esc\,depart\,E2M} = \sqrt{2\left(\frac{\mu_E}{r_{p\,E2M}}\right)} = 10.926 \ \frac{\text{km}}{\text{s}}$$

Equation 10 – To calculate the spacecraft escape velocity from the Earth circular orbit at the periapsis location relative to Earth mass center.

$$v_{\infty\,depart\,E2M} = v_{peri\,E2M} - v_{E/S\,E2M} = 2.945 \ \frac{\text{km}}{\text{s}}$$

Equation 11 – To calculate the hyper excess velocity of the spacecraft on an elliptical transfer trajectory at the edge of Earth's SOI.

The velocity parameter at periapsis for injection into a hyperbolic transfer trajectory is calculated using the following relation in Equation 12 [23].

$$v_{inject\,E2M} = \sqrt{\left(v_{esc\,depart\,E2M}\right)^2 + \left(v_{\infty\,depart\,E2M}\right)^2} = 11.316 \ \frac{\text{km}}{\text{s}}$$

Equation 12 – Calculation of the necessary injection velocity to insert a spacecraft on the Earth-Mars interplanetary transfer.

The velocity necessary to inject onto the hyperbolic trajectory at the Earth periapsis is the difference between this value and the orbital velocity of the spacecraft relative to Earth signifies. This is the tangential burn necessary to inject onto the hyperbolic trajectory.

$$\Delta v_{depart_{E2M}} = v_{inject\,depart_{E2M}} - v_{E\,E2M} = 3.590\ \frac{km}{s}$$

Equation 13 – Total delta-v requirement for the spacecraft to depart on the elliptical Hohmann transfer at Earth periapsis.

The Earth-departure dynamics of the Hohmann transfer are illustrated in Figure 3.
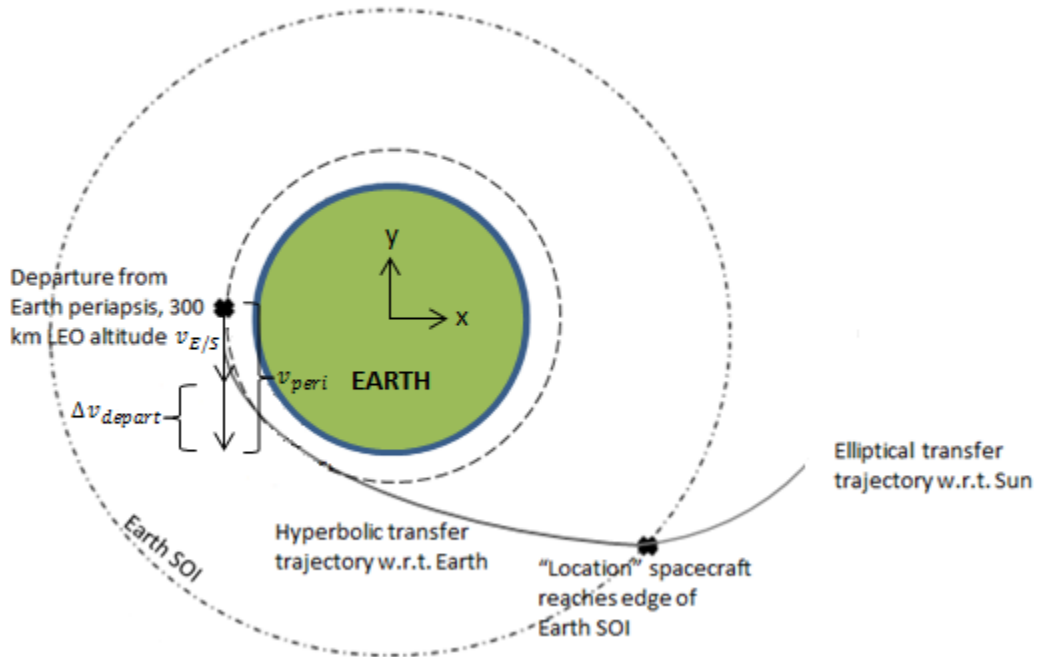
Figure 3 – Illustration of the spacecraft departure trajectory from Earth periapsis at its respected parking orbit altitude. The smaller, dashed circle represents the orbital path of the spacecraft at 300 km altitude relative to the surface of the Earth. The elliptical transfer is conducted at the edge of Earth's SOI upon completion of the hyperbolic transfer trajectory (not drawn to scale).

Under the assumptions for a single tangential burn, the velocity of the spacecraft at apoapsis of the Earth-to-Mars transfer trajectory is found in Equation 14.

$$v_{apo_{E2M}} = \sqrt{2\left(\varepsilon_{E2M} + \left(\frac{\mu_S}{avg_{g_M}}\right)\right)} = 21.478 \ \frac{km}{s}$$

Equation 14 –Velocity of the spacecraft at the Earth-Mars apoapsis prior to LMO insertion.

Taking the difference in the spacecraft orbital velocity about Mars from the velocity at

the apoapsis of the Hohmann transfer from Earth, the hyperbolic excess velocity with

respect to Mars is found in Equation 15.

$$v_{\infty \, arrival_{E2M}} = v_{M/S_{E2M}} - v_{apo_{E2M}} = 2.649 \ \frac{km}{s}$$

Equation 15 –Hyperbolic excess velocity of the spacecraft at the Mars SOI upon arrival following the
Hohmann transfer from Earth periapsis.

In order to determine the necessary velocity impulse to enter circular orbit about Mars,

the escape velocity of the spacecraft with respect to Mars is calculated in Equation 16 and

the periapsis velocity with respect to Mars is calculated in Equation 17.

$$v_{esc \, arrival_{E2M}} = \sqrt{2\left(\frac{\mu_M}{r_{a_{E2M}}}\right)} = 4.826 \ \frac{km}{s}$$

Equation 16 – Escape velocity at Earth apoapsis relative to the planet's mass center.

$$v_{inject \, arrival_{E2M}} = \sqrt{\left(v_{esc \, arrival_{E2M}}\right)^2 + \left(v_{\infty \, arrival_{E2M}}\right)^2} = 5.505 \ \frac{km}{s}$$

Equation 17 – Necessary injection velocity to insert a spacecraft at the Earth apoapsis location into circular
orbit about the planet.

An impulsive maneuver necessary to place the spacecraft at the destined parking altitude

h_M is calculated as the difference between the velocity at periapsis of the Mars-relative

hyperbola and the desired orbital velocity of the spacecraft about the planet at the

required altitude about Mars.

$$v_{M_{E2M}} = \sqrt{\frac{\mu_M}{r_{a_{E2M}}}} = 3.412 \ \frac{km}{s}$$

Equation 18 – Orbital velocity of the spacecraft relative to Mars' mass center at parking orbit altitude, h_M.

$$\Delta v_{arrival_{E2M}} = v_{inject_{arrival_{E2M}}} - v_{M_{E2M}} = 2.093 \ \frac{km}{s}$$

Equation 19 – Differential calculation to determine the total delta-v requirement to enter circular orbit about Mars at the Earth apoapsis location.

The representation for the Mars-arrival dynamics of the Hohmann transfer is illustrated in

Figure 4.
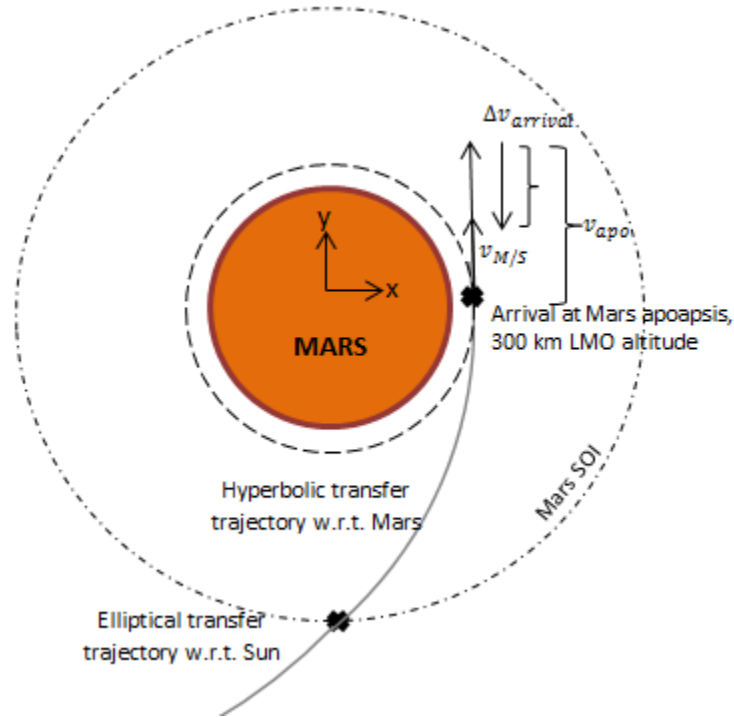
Figure 4 – Illustration of the trajectory design for the spacecraft at Mars arrival. Shown is a depiction of a Hohmann transfer arrival trajectory where transformation to a hyperbolic trajectory is made at the edge of Mars' SOI (not drawn to scale). Parking orbit altitude of the spacecraft about the planet is illustrated by the smallest dashed circle, where injection of the spacecraft into low Martian orbit occurs at periapsis of the hyperbola. The Hohmann transfer places the vehicle ahead of Mars where the planet will "catch up" to the spacecraft. This is known as a Type-II trajectory [38].

To account for drag losses imposed on the rocket during ascension to LEO,

including air frictional drag and gravity, the Δv_{drag} requirement is determined in

Equation 18. The value calculated is based on an empirically observed value of 20%

additional velocity requirement the spacecraft must achieve in order to reach the intended

parking orbit altitude. This velocity value is assumed to be constant for all mission

scenarios that are studied in this paper (the standard deviation among a sample of launch vehicle amounts to about 11%).

$$\Delta v_{drag} = v_{E\,E2M} * 20\% = 1.545\ \frac{km}{s}$$

Equation 20 – Calculation of the additional velocity required by the spacecraft due to drag reduction of the launch delivery vehicle during ascension following launch from Earth. Although the spacecraft orbital velocity around Earth is designated by Earth-to-Mars subscript (*E2M*), the same drag-induced velocity value is used for the rendezvous approach.

The summation of the Δv values for departure and arrival of the spacecraft yields a value that illustrates the necessary propulsive energy required for this scenario. In addition to the Δv values calculated for departure and arrival from Earth and Mars, the energy required to secure the spacecraft about Earth's orbit at the assigned parking orbit as well as the supplementary velocity required in order to account for energy loss due to gravitation and atmospheric drag during launch is considered in this calculation as well. The total Δv for a direct approach via Hohmann transfer to Mars is calculated in Equation 21.

$$\Delta v_{total\,E2M} = \Delta v_{depart\,E2M} + \Delta v_{arrive\,E2M} + v_{E\,E2M} + \Delta v_{drag\,E2M} = 14.954\ \frac{km}{s}$$

Equation 21 – The total velocity required for the Mars-direct mission design approach.

L_2-Lagrange Point Propellant Depot Rendezvous Approach

The alternative profile entails docking a spacecraft at the L_2-Lagrange point for refueling en route to Mars. The analysis demonstrates that an advantage in the required mass is gained from the total Δv maneuvers carried out on this mission profile. The significant advantage for which this analysis proves is that while the necessary total mission propulsive requirements for the rendezvous mission is greater than the direct approach, the advantage lies in the smaller mass delivered to LEO.

32

Mission parameters for the rendezvous approach are assigned in Table 4.

Table 4 – Parking orbit altitudes for both Hohmann transfer phases within the L_2-Lagrange point propellant depot rendezvous approach. Values shown for the E2L2 approach includes the periapsis and apoapsis locations relative to the Earth mass center, while the periapsis of L22M approach is relative to the Earth mass center and the apoapsis is relative to mass center of Mars.

L_2-Lagrange Point Rendezvous Mission Design Approach Initial Parameters		
Mission Phase	**Parameter**	**Value**
E2L2 approach	$r_{p_{E2L2}}$	6,678 km
	$r_{a_{E2L2}}$	444,400 km
L22M approach	$r_{p_{L22M}}$	444,400 km
	$r_{a_{L22M}}$	3,697 km

The overall mission is divided into two approaches, the Earth-to-L_2 approach and the L_2-to-Mars approach. The initial approach for this mission is designed to transport a spacecraft from Earth to the propellant depot at L_2. The secondary approach is designed for post-rendezvous travel from the L_2 position to Mars to deliver the mission payload to the Martian surface.

The initial location of the first tangential burn for departure is located at the periapsis of the Earth-relative elliptical transfer; the apoapsis located at L_2. At this location a second tangential burn is initiated for rendezvous and docking at the propellant station.

$$x_{p_{E2L2}} = avg_E + r_E + h_E = 149,604,701 \text{ km}$$

Equation 22 – Calculation of the periapsis location within the Earth-Moon system relative to the mass center of the Sun.

$$x_{a_{E2M}} = avg_E + avg_{moon} + x_{L2} = 150,042,423 \text{ km}$$

Equation 23 – Calculation of the apoapsis location relative to the Sun mass center within the Earth-Moon system.

The semi-major axis of the transfer within the Earth-Moon system for L_2 rendezvous is the average of the periapsis and apoapsis distances, or the L_2 position (L_2 is located at a radial distance x_{L2} from the Moon's center of mass.

$$a_{E2L2} = \frac{x_{p\,E2L2} + x_{a\,E2L2}}{2} = 225{,}539 \text{ km}$$

Equation 24 – Semi-major axis length within the Hohmann transfer ellipse within the Earth-Moon system.

The orbit's specific mechanical energy is calculated in Equation 25.

$$\varepsilon_{E2L2} = -\frac{\mu_E}{2a_{E2L2}} = -0.884 \frac{\text{km}^2}{\text{s}^2}$$

Equation 25 – Specific orbital energy for the elliptical Hohmann transfer within the Earth-Moon system.

The velocity for which the spacecraft orbits Earth is found in Equation 26.

$$v_{E\,E2L2} = \sqrt{\frac{\mu_E}{r_{p\,E2L2}}} = 7.726 \frac{\text{km}}{\text{s}}$$

Equation 26 – Determination of the orbital velocity of the spacecraft at the 300 km parking orbit altitude within LEO.

Departure on an elliptical Hohmann transfer to L_2 is found by using the specific orbital energy and radial distance of the spacecraft location relative to Earth.

$$v_{peri\,E2L2} = \sqrt{2\left(\varepsilon_{E2L2} + \frac{\mu_E}{r_{p\,E2L2}}\right)} = 10.845 \frac{\text{km}}{\text{s}}$$

Equation 27 – Velocity at Earth-Moon periapsis within the Earth-Moon system.

The departure Δv is taken from the difference in the periapsis and spacecraft orbital velocity relative to Earth, calculated in Equation 28.

$$\Delta v_{depart\,E2L2} = v_{peri\,E2L2} - v_{E\,E2L2} = 3.119 \frac{\text{km}}{\text{s}}$$

Equation 28 – Necessary velocity for spacecraft to initiate Earth departure.

The Earth-departure dynamics of the Hohmann transfer en route to the propellant depot are illustrated in Figure 5.
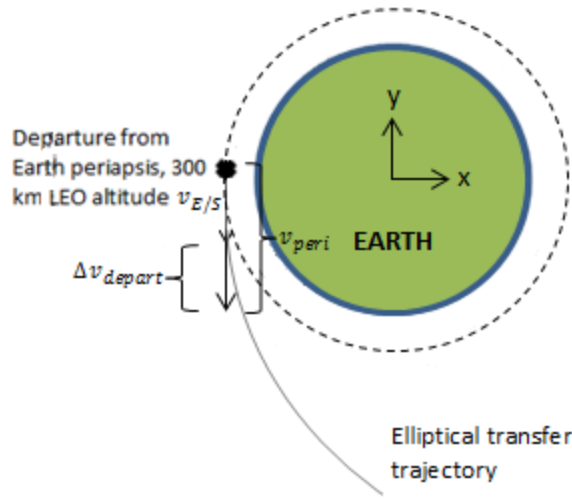
Figure 5 – Illustration of the conic dynamics for a spacecraft departing for the L_2-Lagrange point propellant depot. Located at the periapsis of the Earth-Moon system, the spacecraft departs on a Hohmann transfer to rendezvous at the propellant depot located 60,000 km relative to mass center of the Moon. Unlike the Mars-direct approach, Earth's SOI is not considered illustrated in the figure because it does not bare any significance to demonstrating an elliptical transfer for this stage of the rendezvous mission.

Docking of the spacecraft at the L_2 propellant depot is handled automatically by the vehicle's onboard computers for precision guidance and maneuvering. Upon the assumption that successful docking is achieved between that of the spacecraft and propellant depot, the propellant depot is assumed to be located at the apoapsis location of the Earth-Moon system following transfer. At this location, the velocity for which the spacecraft is traveling relative to the depot is determined in Equation 29.

$$v_{apo_{E2L2}} = \sqrt{2\left(\varepsilon_{E2L2} + \left(\frac{\mu_E}{r_{a_{E2L2}}}\right)\right)} = 0.163 \ \frac{\text{km}}{\text{s}}$$

Equation 29 – Determination of the velocity at the apoapsis location within the Earth-Moon system.

Furthermore, the angular velocity of the spacecraft-depot couple orbiting relative to Earth is calculated in Equation 30, where the angular velocity is required to be determined in order to calculate the velocity of the spacecraft at a distance relative to the Earth.

$$\dot{\theta}_{moon} = \sqrt{\frac{\mu_E}{(avg_{moon})^3}} = 2.649 \text{ x } 10^{-6} \frac{\text{rad}}{\text{s}}$$

Equation 30 – Angular velocity necessary for the spacecraft to travel in conjunction with the propellant depot moving relative to the Moon.

$$v_{L2\dot{\theta}} = (avg_{moon} + x_{L2}) * \dot{\theta}_{moon} = 1.177 \frac{\text{km}}{\text{s}}$$

Equation 31 – Velocity of the spacecraft relative to the mass center of the Earth. The radial distance the propellant depot is located relative to the mass center of the Moon, x_{L2}, is 60,000 km.

The propulsive impulse for the spacecraft to rendezvous with the propellant depot is

determined in Equation 32.

$$\Delta v_{L2rendezvous} = v_{L2\dot{\theta}} - v_{apo_{E2L2}} = 1.014 \frac{\text{km}}{\text{s}}$$

Equation 32 – Propulsive impulse of the spacecraft to rendezvous at the propellant depot.

Departure on a Hohmann transfer to Mars is the secondary stage of the mission.

The departure maneuver is implemented at a position away from the depot following

undocking. The propulsive perturbations for this maneuver, however, are not considered

in the total energy necessary for the mission. Similar to patched conic approximation

implemented in the Mars-direct approach, departure from the propellant depot at the

periapsis location of the Hohmann transfer uses a hyperbolic departure maneuver in order

to escape Earth's gravitation influence. Departure from the L_2-Lagrange propellant depot

requires a hyperbolic trajectory prior to the elliptical transfer within the Moon-Mars

Hohmann transfer, which considers the same approach of the spacecraft departing on a

hyperbolic trajectory from Earth because the location of departure at the depot still lies

within Earth's SOI.

$$v_{\infty depart_{L22M}} = v_{peri_{E2M}} - v_{E/S_{E2M}} = 2.945 \frac{\text{km}}{\text{s}}$$

Equation 33 – Hyperbolic excess velocity calculated at the edge of Earth's SOI, which is determined to reach just beyond the propellant depot at the L_2-Lagrange point with the Earth-Moon system.

The escape velocity relative to Earth is calculated in order to determine the velocity change necessary to inject on to a Hohmann transfer to Mars,

$$v_{esc\,depart_{L22M}} = \sqrt{2\left(\frac{\mu_E}{avg_{moon}+x_{L2}}\right)} = 1.339\,\frac{km}{s}$$

Equation 34 – Escape velocity of the spacecraft departing the propellant depot at the periapsis location of the Moon-Mars system. The spacecraft is considered to still be within Earth's gravitation influence because the propellant depot location lies within the planet's SOI region.

$$v_{inject\,depart_{L22M}} = \sqrt{\left(v_{\infty\,depart_{L22M}}\right)^2 + \left(v_{esc\,depart_{L22M}}\right)^2} = 3.235\,\frac{km}{s}$$

Equation 35 – Injection velocity required for the spacecraft to insert the Hohmann transfer en route to Mars.

The total velocity change necessary to initiating the departure maneuver is found, which takes the difference of the spacecraft injection departure velocity from the L_2-Lagrange point propellant depot and the spacecraft-depot couple velocity.

$$\Delta v_{depart_{L22M}} = v_{inject\,depart_{L22M}} - v_{L2_{\dot\theta}} = 2.058\,\frac{km}{s}$$

Equation 36 – Propulsive requirement of the spacecraft to depart the L_2-Lagrange point propellant depot.

The final phase of the transfer commences with the arrival of the spacecraft at the edge of Mars' SOI. In this region, reference to the Sun is taken into consideration when determining the hyperbolic excess velocity the spacecraft is experiencing as it approaches Mars' SOI prior to penetrating the region's 'edge'.

$$v_{\infty\,arrival_{L22M}} = v_{M/S_{L22M}} - v_{apo_{E2L2}} = 2.648\,\frac{km}{s}$$

Equation 37 – Hyperbolic excess velocity at the edge of Mars' SOI, however, considered under the gravitation influence of the Sun. Hyperbolic velocity of the spacecraft at arrival is determined by the differential in the known velocities at apoapsis of the Moon-Mars system and the orbital velocity of the spacecraft relative to the distance from Mars' mass center.

The escape velocity of the spacecraft, relative to the summation of the planetary radius of Mars and the parking orbit altitude in LMO, is found.

$$v_{esc\,arrival_{L22M}} = \sqrt{2\left(\frac{\mu_M}{r_{a_{E2L2}}}\right)} = 4.826 \ \frac{\text{km}}{\text{s}}$$

Equation 38 – Calculation of the escape velocity in order to determine the injection velocity required by the spacecraft to insert into circular about Mars.

Injection of the spacecraft on a trajectory to enter a circular orbit about Mars at a parking orbit h_M is calculated in Equation 40.

$$v_{inject\,arrival_{L22M}} = \sqrt{\left(v_{\infty\,arrival_{L22M}}\right)^2 + \left(v_{esc\,arrival_{L22M}}\right)^2} = 5.505 \ \frac{\text{km}}{\text{s}}$$

Equation 39 – Injection velocity to insert spacecraft in Mars circular orbit based on a single tangential burn at Mars apoapsis.

Finally, the propulsive energy required for the spacecraft to enter LMO is found in Equation 40.

$$\Delta v_{arrival_{L22M}} = v_{inject\,arrival_{L22M}} - v_{M\,L22M} = 2.092 \ \frac{\text{km}}{\text{s}}$$

Equation 40 – Required propulsive energy by the spacecraft for insertion into Mars circular orbit, based on the difference in the injection velocity and velocity required to maintain the spacecraft in circular orbit about the planet.

The summation of the Δv values for departure and arrival of the spacecraft requires the determination of those values for both stages of the mission, a Hohmann transfer each for the Earth-Moon transfer and the Moon-Mars transfer. The total Δv for a rendezvous approach by way of an L_2-Lagrange point propellant station via Hohmann transfer to Mars is calculated in Equation 41.

$$\Delta v_{total_{L2rendezvous}} = \Delta v_{depart_{E2L2}} + \Delta v_{L2rendezvous} + \Delta v_{depart_{L22M}}$$

$$+\Delta v_{arrival_{L22M}} + v_{E\,E2L2} + \Delta v_{drag} = 17.554 \ \frac{\text{km}}{\text{s}}$$

Equation 41 – Total velocity requirements for the spacecraft based on the propulsive requirements for Earth departure, rendezvous and departure at the L_2-Lagrange point propellant depot, and arrival at Mars.

The representation for the arrival and departure dynamics at the L_2-Lagrange point propellant depot is illustrated in Figure 6.
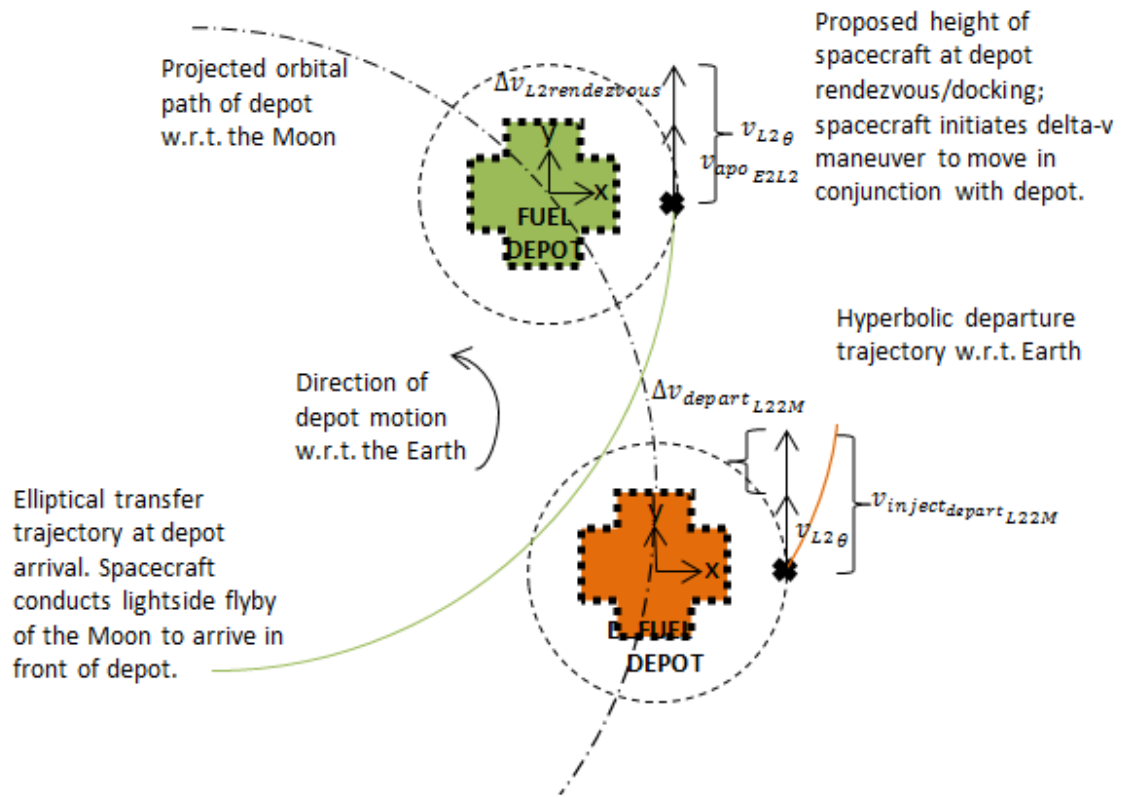
Figure 6 – The green trajectory represents the spacecraft arriving in front of the propellant depot, which is located at the Earth apoapsis of the interplanetary transfer. Initiating this maneuver requires the spacecraft to impose a propulsive change in its trajectory in order for the depot to essentially rendezvous with the spacecraft. The orange trajectory illustrates the departure trajectory of the spacecraft en route to Mars where it departs from the propellant depot. The dashed line around the propellant depots illustrates the edge where either automatic docking or undocking of the spacecraft with the depot occurs prior to arrival/departure.

Payload Transfer Vehicle

Nations around the globe are researching more ways to explore space than ever before. These alternative payload delivery methods will be investigated primarily to reduce total mission costs. Current launch systems which dump spent vehicle stages may become a thing of the past as more programs are looking to use pre-existing launch vehicle components and adopt stage reusability as integral aspects of future mission designs [39]. Companies are exploring new methods for extending versatility of their

vehicle hardware, specifically within the focus of vehicle stage reusability or secondary mission objectives. This includes utilizing segments presently available on existing launch vehicles as well as other preliminary vehicle designs from other programs such as upper/second stage vehicles.

There have been numerous mission scenarios designed with the intention of using launch vehicle components specifically for flight missions or space habitats. One example is the Lunar CRater Observation and Sensing Satellite (LCROSS)/Lunar Reconnaissance Orbiter (LRO) dual-payload mission conducted in 2009. By utilizing the Centaur EDUS (Earth Departure Upper Stage) of the Atlas V launch vehicle, engineers designed the secondary stage of the rocket to perform two extended mission operations beyond what the segment was initially intended for [39]. The design of the Centaur accomplished multiple mission objectives within a single spacecraft, which included the transfer of both payloads to the Moon and kinetic impactor for the LCROSS payload to analyze regolith moisture levels upon Centaur impact on the lunar surface. The uniqueness of the mission served as a prime example of the innovative methods programs are now seeking in order to utilize all resources within the mission, both optimizing versatility as well as minimizing costs. This same concept, utilizing an upper stage for the purpose of payload transfer, was considered as a design option for the two mission design scenarios being explored by the primary investigator.

The payload transfer vehicle is considered as the primary spacecraft to transport the mission payload from LEO to LMO where it is deployed into the Martian atmosphere for the landing phase of the mission. Initiation of the mission's transfer vehicle phase begins upon separation from the launch delivery vehicle booster(s) upon ascension from

Earth atmosphere and will continue through a calculated coast time, dependent on the specific mission arrival/rendezvous location. This was the approach adopted by the Centaur EDUS during the LCROSS/LRO mission, which conducted an additional 23-minute coast burn upon achieving LEO [39].

Atlas V Common Centaur

The Atlas V 400 and 500 series launch vehicle evolved from a long lineage of Atlas family spacecraft. Both vehicle series were put into service in 2002. Current configurations of the Atlas V vehicle uses a standard Atlas booster, zero to five solid rocket boosters (SRBs), a Centaur transfer vehicle (either a single engine centaur (SEC) or dual engine centaur (DEC) configurations), and composite payload fairing (PLF). The three-digit identification for vehicle configuration stands for, in order, the payload fairing diameter (in meters), the total number of SRBs, and the total number of Centaur engines on the second stage of the rocket [40].

The Atlas V second stage, known as the Common Centaur, is powered by either one or two Pratt & Whitney RL-10A-4-2 engines. Selection for the SEC or DEC system is based on the payload transfer and deployment requirements for the launch vehicle to meet. The RL-10A-4-2 engine has the capability for multiple in-space starts, which makes it possible for such applications as LEO and GTO insertion within a single mission with a planned coast period in-between [41].

Delta IV Delta Cryogenic Second Stage

The Delta launch vehicle has a long heritage within space launch vehicle

programs dating back to the 1950s. First initiated by NASA as a modified Thor missile

with Vanguard second and third stages, the Delta family currently consists of two launch

vehicle systems: the Delta II and the Delta IV. The newest member of the family, the

Delta IV comes in three vehicle configurations: the Delta IV-Medium (Delta IV-M),

three variants of the Delta IV-Medium-Plus (Delta IV-M+), and the Delta Heavy (Delta

IV-H) [42].

Although a Delta IV-M configuration does not include any solid rocket motors

(SRMs) to augment its first stage CBC, the Delta IV-M+ can be equipped with two or

four SRMs. The three Delta IV-M+ variants are the Delta IV-M+ (4,2), Delta IV-M+

(5,2), and Delta IV-M+ (5,4); the first digit in the parenthesis refers to the diameter of the

second stage in meters, the second digit representing the total number of SRMs

configured to the first stage CBC. The Delta IV-M+ (4,2) utilizes a 4-m diameter

composite PLF while the Delta IV-M+ (5,2) and Delta IV-M+ (5,4) employ a 5-m

diameter composite PLF. The Delta IV-H may be configured either with a 5-m metallic

PLF or 5-m composite PLF [42].

Each Delta IV is equipped with a newly manufactured first stage, known as the

Common Booster Core (CBC). In the case of the Delta IV-H, the vehicle is equipped

with three first-stage CBCs to supplement additional thrust requirements for a high-mass

payload. Each CBC is powered by a liquid hydrogen/liquid oxygen consuming

Rocketdyne RS-68 engine, designed to perform at a 102% rated thrust level with a

throttle-down capability approaching a 58% rated thrust level. All three Delta IV variants

are configured with a Delta Cryogenic Second Stage (DCSS) with a single RL-10B-2 engine. Each Delta IV has an identical second stage dependent on the diametrical size of the vehicle's CBC diameter [42].

SpaceX Falcon 9 Stage 2

Space Exploration Technologies Corporation (SpaceX), founded in 2002, is a privately-funded space-launch services company. In 2006, NASA awarded SpaceX with a Commercial Orbital Transportations Services (COTS) to design and demonstrate a space launch system capable of providing cargo resupply capabilities to the ISS, as well as a potential crew transport option [43]. With the incorporation of milestone incentives within the contract to meet certain design and mission objectives, NASA awarded SpaceX won a Commercial Resupply Services (CRS) contract, which included twelve missions to the ISS for cargo and supplies to the orbital outpost and crew onboard [68]. The first CRS mission was accomplished in May 2012, making SpaceX the first private company to send a cargo payload to the ISS [44].

The Falcon family is comprised of three launch vehicles: the Falcon 1, Falcon 9 version (v) 1.0, and future Falcon Heavy. The Falcon 9 is the only active rocket currently used in the fleet. Development is underway for upgrades to the Falcon 9 propulsion system. The Merlin 9 v1.1 will incorporate an enhanced Merlin 1D engine, which will provide greater lifting capability to transport larger liftoff masses to LEO and GEO. The newly redesigned engine will have the ability to throttle down from 100% to 70% compared to the currently used Merlin 1C model. The vacuum version of the Merlin 1D

engine is planned for use on the Falcon Heavy second stage with a specific impulse value of 311 s [45].

Mass Requirements per Mission Design Approach

In order to determine the propellant, empty, and overall gross mass requirements for each mission design scenario (see Appendix for derivation of processes for calculation), the specific impulse parameter is defined by the propulsion system utilized within each payload transfer vehicle. These propulsion systems are described in Table 5 [46]. The product of the specific impulse value of the vehicle and the Earth gravitation acceleration constant is simplified to a common term, the exhaust velocity ($c_{vehicle}$), applied when calculating the propellant mass values. Due to current materials technology, a lower limit of 0.10 is chosen as a constant value for the structural ratio value (ϵ) when calculating the empty mass quantities [24].

Table 5 – Shown are the propulsion system specifications for each upper/second stage vehicle under investigated for potential use as a future payload transfer vehicle.

Propulsion Systems for Active Upper/Second Stages				
Vehicle	**Engine Type**	**Fuel Type**	**Specific Impulse**	**Vehicle Allocations**
United Launch Alliance – Common Centaur Upper Stage	Pratt & Whitney Rocketdyne RL-10A4-2 Liquid-Fuel Cryogenic Engine	LH2/LOX	451 s	• Atlas V 400 & 500 series rockets
United Launch Alliance – DCSS	Pratt & Whitney Rocketdyne RL-10B-2 Liquid-Fuel Cryogenic Engine	LH2/LOX	462 s	• Delta IV rockets* • SLS Block I stage
SpaceX – Stage 2	SpaceX Merlin 1D Engine	LOX/RP-1**	311 s	• Falcon 9 v1.1***
Note: *4-m fairing incorporates a one engine DCSS design; 5-m fairing uses two RL-10B-2 engines **Rocket-grade kerosene ***Falcon 9 v1.1 to be flown late 2013				

Entry, Descent, & Landing Phase

The capability for a payload to land on the Martian surface is an exceedingly difficult task to undertake. Entry, descent, and landing (EDL) is a high risk challenge for delivering the payload to a precise location under a plethora of constraints and environmental variables. The vehicle must be designed with sufficient thermal protection for vehicle entry due to the thin Martian atmosphere as well as a supersonic retrograde propulsion system to decelerate the entry vehicle prior to landing on the ground [47].

The Mars-optioned shroud, a Mars payload /vehicle delivery concept initially designated for the Ares V launch vehicle, is utilized as the primary design of the payload encapsulation structure which is mounted directly to the payload transfer vehicle of the launch delivery vehicle. Although the shroud was intended primarily for the Ares V launch vehicle, it shares similar design characteristics from its initial Ares V design while adopting those technologies associated with the new payload fairings of SLS. The SLS payload fairing, a 25-m x 8.38-m encapsulation structure, incorporates a standard bi-conic shroud design with a total structural mass of 12,110 kg (Figure 7) [48].

Figure 7 – The Mars multi-use shroud option is comprised of a thickened composite sandwich material to provide micro-meteorite protection and an ablative thermal protection surface [49]. Utilization of composite materials will also minimize overall mass, thus, propellant requirements for the launch vehicle. The TPS (illustrated as black in the figure) provides thermal loading protection during entry and descent en route to deploying that mission payload to the Martian surface.

This large encapsulation structure serves three main functions: 1) Earth-ascent payload encapsulation, 2) Orbital-transfer protection, 3) Planetary thermal protection for payload delivery. Normally, payload shrouds are discarded upon ascent out of Earth's atmosphere; however, the multi-use shroud is strengthened to provide micro-meteorite protection, cosmic radiation payload protection during the Earth-Mars transfer, and aero-thermal protection during EDL. The rigid aeroshell is also equipped with a supersonic retrograde propulsion system, which provides the vehicle the ability to exercise precision controls for maneuvering and landing on the Martian surface. The shroud enters through the Martian atmosphere, jettisoning the habitat from encapsulation structure when reduction in the entry velocity has diminished to the intended amount. From here, the habitat initiates a retrograde descent maneuver to control vehicle orientation and translation en route to the landing site.

A vehicle entering the atmosphere at such a high rate of speed requires a deceleration technique to be accomplished in under two minutes. Previous lander mission entering the Martian atmosphere have traveled at hypersonic entrance velocities of Mach 2, 3 and 4. Two methods for decreasing the shroud's entry velocity were considered: 1) a parachute design, one in which requires zero fuel necessary for vehicle entry velocity reduction; 2) a retrograde propulsion system, which requires propellant mass for power. The implementation of a retrograde propulsion system was chosen as the primary technique to minimize the vehicle's descent velocity. A parachute required both a large chute diameter to decrease the hypersonic entry velocity of the vehicle as well as a large timeline for the chute to open, two disadvantages to the overall mission objective [47].

Previous analysis conducted on the 10-m x 30-m shroud found a landing velocity parameter on Mars at approximately 1.23 km/s, which includes a 265 m/s cross range maneuver to orient the vehicle correctly for landing during descent. As shown in Figure 8, landing the mission payload on the Martian surface is based on the vehicle mass and the required propulsive energy to descend the payload to the surface. The low ballistic coefficient of the shroud, while penetrating through the atmosphere, indicates that a high negative acceleration is required. This is under the assumption that the vehicle entering the atmosphere is of small volume which typically signifies a small surface area entering the atmosphere (the orientation of the vehicle entering the atmosphere (nose-first or length-wise of the vehicle) will have an effect on the vehicle's deceleration rate). Therefore, the vehicle requires a greater Δv to decelerate during descent [26, 47].

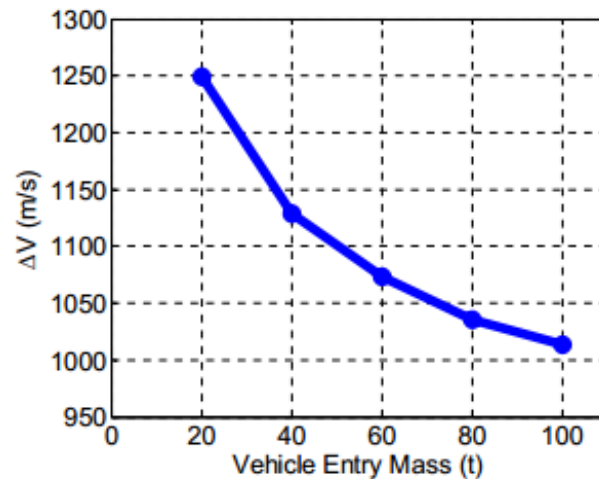Figure 8 – Mars EDL phase relating vehicle entry mass with the gross propulsive energy velocity requirement for decelerating a vehicle from Mach 3 [47].

Using the known payload mass value values, as well as the exhaust velocity of the mission payload ($c_{P/L}$) and a vehicle structural ratio value of 0.10, a preliminary fuel mass requirement for the habitat's retrograde propulsion systems is calculated, shown in

Equation 42 [50]. Specifically for the landing phase of the mission, the mission payload

mass and the payload empty mass values are different. The mission payload mass $(m_{P/L})$

represents the structural mass of the habitat while the empty mass required for the landing

phase of the mission $(m_{e\,land})$ is mass necessary to support propulsion system mass and

its associated propellant mass.

$$m_{P\,land} = m_{P/L}\left(\frac{(1-\epsilon)\left(e^{\frac{\Delta v_{land}}{c_{P/L}}}-1\right)}{\left(1-\epsilon e^{\frac{\Delta v_{land}}{c_{P/L}}}\right)}\right) = 8{,}794.56 \text{ kg}$$

Equation 42 – Propellant mass required by the mission payload to land on the Martian surface.

The empty mass of the vehicle during the landing phase of the mission is determined in

Equation 43.

$$m_{e\,land} = \left(\frac{\epsilon}{1-\epsilon}\right)m_{P\,land} = 977.17 \text{ kg}$$

Equation 43 – Empty mass required to support the necessary propellant mass for landing of the mission payload.

The gross mass value of the habitat, which includes the required propellant, support

structures, and propulsion system masses necessary for supporting the landing phase of

the mission, is calculated in Equation 44.

$$m_{0\,land} = m_{P\,land} + m_{e\,land} + m_{P/L} = 34{,}771.74 \text{ kg}$$

Equation 44 – Calculation of the gross mass quantity for the mission landing phase.

The entry and descent phase of the mission is initiated upon penetration of the

shroud, comprised of the habitat payload encapsulated within the structure, through the

Martian atmosphere. Aerobraking allows the spacecraft to reduce velocity upon orbital

entry at Mars, decelerating the vehicle without the large necessity of fuel required.

Aerobraking is initiated following circularization of the spacecraft's orbit around the

planet. Because of Mars' thin atmosphere, the spacecraft conducts several orbital passes

around the planet, where the mass of the Martian body pulls the spacecraft closer into

outer levels of its atmosphere. As the spacecraft makes several passes through the thin

atmosphere, slowing the spacecraft down to where it is practically captured within the

atmosphere, falling to the surface for landing [51].

LMO Injection Phase

Injection into the circularization about the Martian planetary body incorporates

the inclusion of the calculated gross masses of the habitat and the shroud for the EDL

phases of the mission. The integration of these two masses is intended to be integrated

with the payload transfer vehicle for both the Mars-direct approach and L_2-Lagrange

point rendezvous approach. The insertion velocity into LMO for the spacecraft

transferring from LEO is 2.09 $\frac{\text{km}}{\text{s}}$ (rounded value), found in previous calculations. The

propellant requirement for a single payload transfer vehicle is dependent on the specific

impulse and the vehicle mass. Using this parameter as the independent variable, the

propellant requirement for spacecraft orbital injection about Mars for either the Mars-

direct approach or L_2-Lagrange rendezvous approach is found using Equation 45 for each

type of propulsions system under investigation.

$$m_{P\,inject_{vehicle}} = m_{0_{land}} \left(\frac{(1-\epsilon)\left(e^{\frac{\Delta v_{arrival_{E2M}}}{c_{vehicle}}} - 1 \right)}{\left(1-\epsilon e^{\frac{\Delta v_{arrival_{E2M}}}{c_{vehicle}}} \right)} \right)$$

Equation 45 – Propellant mass requirement, with inclusion of the shroud mass within the gross mass
quantity within the landing phase ($m_{0_{land}}$), for injection into LMO based on the arrival velocity of the
spacecraft at apoapsis of the Moon-Mars system.

Upon calculation of the propellant mass value for each upper/second stage, the empty

structural mass is calculated in Equation 46.

$$m_{e\,inject_{vehicle}} = \left(\frac{\epsilon}{1-\epsilon}\right) m_{P\,inject_{vehicle}}$$

Equation 46 – To calculate the empty mass required to support the necessary propellant mass for the entry
phase of the vehicle into LMO.

Calculation of the gross vehicle mass being injected into LMO, which includes the

summation of the propellant mass, empty mass and gross mass being delivered for the

landing phase of the mission, is determined in Equation 47.

$$m_{0\,inject_{vehicle}} = m_{P\,inject_{vehicle}} + m_{e\,inject_{vehicle}} + m_{0\,land}$$

Equation 47 – Calculation for the gross mass quantity of vehicle injection into LMO.

The results are presented in Table 6.

Table 6 – Propellant mass, empty mass, and gross masses to inject in to Mars LMO based on the velocity
requirement at arrival to Mars and propulsion system exhaust velocity. The gross mass values include the
necessary propellant and empty mass values for the landing phase of the mission, as well as those same
values for injection in LMO, as shown in Equation 47 as well.

Staging Values for Injection into LMO			
Propulsion System	$m_{P\,inject_{vehicle}}$	$m_{e\,inject_{vehicle}}$	$m_{0\,inject_{vehicle}}$
ULA – Common Centaur Upper Stage RL-10A4-2	30,384.03 kg	3,376.00 kg	80,631.77 kg
ULA – DCSS RL-10B-2	29,418.24 kg	3,268.69 kg	79,558.67 kg
SpaceX – Falcon 9 Stage 2 Merlin 1D	51,866.19 kg	5,762.91 kg	104,500.83 kg

Mars-Direct Approach

The total propellant mass requirements for both the Mars-direct approach and L_2-

Lagrange point propellant depot rendezvous approach is found using the three different

specific impulse parameters listed in Table 5. The Mars-direct approach takes into

consideration delivery of the calculated 'payload' mass, consisting of the propellant,

empty mass, and mission payload required for landing and orbital injection from Earth-

LEO to arrival at Mars' SOI. A single payload transfer vehicle is used within the analysis

of the three upper/second stages under investigation.

Prior to initiation of vehicle aerobraking following circular orbit injection about

Mars, the propellant mass required for the transfer vehicle to travel from the parking orbit

altitude about Earth from the departure point at periapsis is calculated in Equation 48.

$$m_{P_{vehicle\,E2M}} = m_{0_{inject}} \left(\frac{(1-\epsilon)\left(e^{\frac{\Delta v_{depart_{E2M}}}{c_{vehicle}}} - 1 \right)}{\left(1 - \epsilon e^{\frac{\Delta v_{depart_{E2M}}}{c_{vehicle}}} \right)} \right)$$

Equation 48 – To calculate the propellant mass requirement per each payload transfer vehicle's propulsion system for the Earth-to-Mars transfer.

The $\Delta v_{depart_{E2M}}$ quantity is the departure velocity of the transfer vehicle from Earth

periapsis to arrival at Mars' SOI. The empty structural mass is calculated in Equation 49.

$$m_{e_{vehicle\,E2M}} = \left(\frac{\epsilon}{1-\epsilon} \right) m_{P_{vehicle\,E2M}}$$

Equation 49 – Empty mass required to support the necessary propellant mass for the transfer phase from LEO to LMO for the Mars-Direct approach.

The gross vehicle mass encompassing the total vehicle mass for landing and LMO-

injection for vehicular orbit about Mars is calculated in Equation 50.

$$m_{0_{vehicle\,E2M}} = m_{P_{vehicle\,E2M}} + m_{e_{vehicle\,E2M}} + m_{0_{inject_{vehicle}}}$$

Equation 50 – Gross mass quantity to support the upper/second stage-specific propulsion system for the transfer phase from LEO to LMO.

Table 7 – Propellant mass, empty mass, and gross mass values required for a spacecraft to reach Mars LMO from the Earth-Mars system periapsis. The gross mass values include the necessary propellant and empty mass values for the landing and LMO injection phases, as well as the necessary propellant and empty mass values for the Earth-to-Mars stage. This is shown in Equation 50.

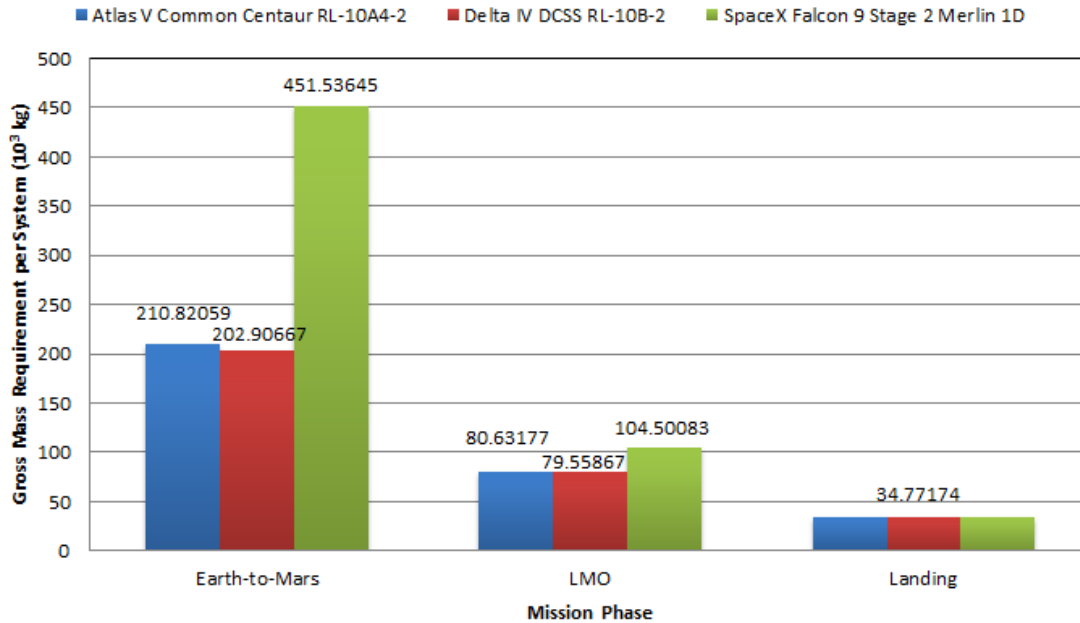| Staging Values for Mars-Direct Approach from LEO Parking Orbit Altitude			
Propulsion System	$m_{P_{vehicle\,E2M}}$	$m_{e_{vehicle\,E2M}}$	$m_{0_{vehicle\,E2M}}$
ULA – Common Centaur Upper Stage RL-10A4-2	117,169.94 kg	13,018.88 kg	210,820.59 kg
ULA – DCSS RL-10B-2	111,013.20 kg	12,334.80 kg	202,906.67 kg
SpaceX – Falcon 9 Stage 2 Merlin 1D	312,332.06 kg	34,703.56 kg	451,536.45 kg

Figure 9 - Gross mass requirements per each phase within the Mars-direct mission. Shown are the necessary values to support the propulsion systems for each payload transfer vehicle.

L2-Lagrange Point Fuel Depot Rendezvous Approach

The propellant mass determination for the L_2 rendezvous mission design scenario
is calculated for the two stages previously defined. The L_2-to-Mars stage (Equation 51) is
handled as the principal parameter for calculating the preceding Earth-to-L_2 stage of the
complete mission. A single payload transfer vehicle is used within the analysis of the
three upper/second stages under investigation.

$$m_{P_{vehicle\,L22M}} = m_{0_{inject_{vehicle}}} \left(\frac{(1-\varepsilon)\left(e^{\frac{\Delta v_{depart_{L22M}}}{c_{vehicle}}} - 1 \right)}{\left(1 - \varepsilon e^{\frac{\Delta v_{depart_{L22M}}}{c_{vehicle}}} \right)} \right)$$

Equation 51 – To calculate the propellant mass requirement for the L_2-to-Mars phase of the rendezvous
approach. The determined value is based on the performance parameters for each vehicle's propulsion
system.

The $\Delta v_{depart_{L22M}}$ quantity represents the required velocity of the payload transfer
vehicle to depart from the L_2-Lagrange point propellant depot and arrive at Mars' SOI in
order to initiate the necessary hyperbolic transfer trajectory to transfer to the Moon-Mars
apoapsis.

Using this propellant mass value, the empty structure parameter, which is
comprised of the propulsion system structure, engine, and fuel tanks, as well as controls
systems for the vehicle pneumatics/hydraulics, is determined for the L_2-to-Mars approach
in Equation 52. This empty mass parameter is calculated for each upper/second stage
under investigation within this approach.

$$m_{e_{vehicle\,L22M}} = \left(\frac{\epsilon}{1-\epsilon} \right) m_{P_{vehicle\,L22M}}$$

Equation 52 – Empty mass required to support the necessary propellant mass for the transfer phase from the
L_2-Lagrange point propellant depot to LMO for the L_2-rendezvous approach.

The gross mass value for the L_2-to-Mars stage, including the previously determined

parameters determined for the LMO-injection and landing phases at the end of the

approach, is found in Equation 54.

$$m_{0_{vehicle_{L22M}}} = m_{P_{vehicle_{L22M}}} + m_{e_{vehicle_{L22M}}} + m_{0_{inject_{vehicle}}}$$

Equation 53 –Gross mass quantity to support the upper/second stage-specific propulsion system for transfer from the L_2-Lagrange point propellant depot to LMO.

The results for the L_2-to-Mars approach for each payload transfer vehicle propulsion

system are shown in Table 8.

Table 8 – Propellant mass, empty mass, and gross mass values required for a spacecraft to reach Mars LMO from the L_2-Lagrange point propellant depot located at the periapsis of the Moon-Mars system. The gross mass values include the necessary propellant and empty mass values for the landing and LMO injection phases, as well as the necessary propellant and empty mass values for the L_2-to-Mars stage. This is shown in Equation 53.

Staging Values from the L2-Lagrange Point Propellant Depot to LMO			
Propulsion System	$m_{P_{vehicle_{L22M}}}$	$m_{e_{vehicle_{L22M}}}$	$m_{0_{vehicle_{L22M}}}$
ULA – Common Centaur Upper Stage RL-10A4-2	51,114.93 kg	5,679.44 kg	137,426.14 kg
ULA – DCSS RL-10B-2	48,839.41 kg	5,426.60 kg	133,824.68 kg
SpaceX – Falcon 9 Stage 2 Merlin 1D	112,701.44 kg	12,522.38 kg	229,724.66 kg

The uniqueness of implementing a rendezvous approach en route to Mars versus a

direct approach is the minimization of the unnecessary transfer of propellant mass and

empty mass to LEO. Incorporating a propellant depot at the L_2-Lagrange point eliminates

the necessity for the gross mass for the direct approach to be loaded onto a launch

delivery vehicle. Instead, by incorporating an intermission rendezvous location, the

capability for a spacecraft to have access to an additional fuel resource is an advantage in mission designs.

Determination of the fuel mass required to complete the rendezvous approach at the L_2-Lagrange point propellant depot takes into consideration the mass parameters determined for the injection in LMO and landing phases of the mission. However, the propellant masses associated with these phases are not considered in the Earth-to-L_2 approach because those vehicles are intended to remain empty prior to vehicular refueling at the L_2-Lagrange point propellant depot. The only necessary mass parameters that are considered include the empty structural masses of the payload transfer vehicle, the shroud, and the mission payload to be delivered to the Martian surface. The required propellant mass necessary for rendezvous of the spacecraft is calculated in Equation 54.

$$m_{P_{vehicle\,L2rendezvous}} =$$

$$(m_{0_{inject\,vehicle}} - m_{P_{vehicle\,L22M}} - m_{P_{inject\,vehicle}} - m_{P_{land}}) \left(\frac{(1-\epsilon)\left(e^{\frac{\Delta v_{L2rendezvous}}{c_{vehicle}}} - 1 \right)}{\left(1 - \epsilon e^{\frac{\Delta v_{L2rendezvous}}{c_{vehicle}}} \right)} \right)$$

Equation 54 – To calculate the propellant mass requirement for the rendezvous phase at the L_2-Lagrange point propellant depot. The necessary fuel requirements for the L_2-to-Mars phase, injection into LMO, and landing are not included because the spacecraft will upload the necessary fuel masses upon rendezvous at the depot; fuel masses for the L_2-to-Mars stage of the rendezvous approach will not be stored within the vehicle for launch from Earth.

Using the known propellant mass value, the empty structural mass to support the propulsion system for rendezvous is calculated in Equation 55.

$$m_{e_{vehicle\,L2rendezvous}} = \left(\frac{\epsilon}{1-\epsilon} \right) m_{P_{vehicle\,L2rendezvous}}$$

Equation 55 – Empty mass required to support the necessary propellant mass for the rendezvous phase at the L_2-Lagrange point propellant depot.

Finally, the known mass parameters, inclusive to that of the mission payload, are combined to define the gross mass value required to support each payload transfer vehicle's propulsion system, which is calculated in Equation 56.

$$m_{0\,vehicle\,L2rendezvous} = m_{P\,vehicle\,L2rendezvous} + m_{e\,vehicle\,L2rendezvous} + m_{e\,vehicle\,L22M} +$$

$$m_{e\,vehicle\,inject} + m_{e\,land} + m_{shroud} + m_{P/L}$$

Equation 56 – Gross mass value including the empty mass parameters for the L_2-to-Mars phase, LMO injection phase, and landing for the rendezvous phase at the L_2-Lagrange point propellant depot. The calculation also includes the masses of the shroud and the mission payload because these structures will be transported with the spacecraft during all phases of the rendezvous mission.

The mass values for rendezvous at the L_2-Lagrange point propellant depot is shown in Table 9.

Table 9 – Propellant mass, empty mass, and gross mass values required for a spacecraft to rendezvous at the L_2-Lagrange point propellant depot at apoapsis within the Earth-Moon system. The spacecraft is traveling from its departure point, located at h_E. The gross mass values include the only the necessary empty mass values for the landing and LMO injection phases, as well as the necessary propellant and empty mass values for rendezvous at the L_2-Lagrange point propellant depot. This is shown in Equation 56.

Staging Values for Rendezvous at L_2-Lagrange Point Propellant Depot			
Propulsion System	$m_{P\,vehicle\,L2rendezvous}$	$m_{e\,vehicle\,L2rendezvous}$	$m_{0\,vehicle\,L2rendezvosu}$
ULA – Common Centaur Upper Stage RL-10A4-2	12,502.06 kg	1,389.18 kg	61,023.79 kg
ULA – DCSS RL-10B-2	12,067.44 kg	1,340.83 kg	60,180.73 kg
SpaceX – Falcon 9 Stage 2 Merlin 1D	23,247.12 kg	2,583.01 kg	82,192.60 kg

Transit to the propellant depot located within the Earth-Moon system requires consolidation of the propellant mass and empty mass necessary to support each payload transfer vehicle's propulsion system for rendezvous at the L_2-Lagrangian point. Assuming that no propellant mass is launched within the spacecraft prior to the L_2-to-Mars transfer stage, which includes those masses required for the LMO-injection and landing phase, the propellant mass required for the Earth-to-L_2 phase of the rendezvous mission design approach is found in Equation 57.

$$m_{P_{vehicle\,E2L2}} = m_{0_{vehicle\,L2rendezvous}} \left(\frac{(1-\epsilon)\left(e^{\frac{\Delta v_{depart_{E2L2}}}{c_{vehicle}}} - 1 \right)}{\left(1 - \epsilon e^{\frac{\Delta v_{depart_{E2L2}}}{c_{vehicle}}} \right)} \right)$$

Equation 57 – To calculate the propellant mass requirement for the Earth-to-L_2 phase of the rendezvous approach. The determined value is based on the performance parameters for each vehicle's propulsion system.

The empty structural mass to support the propulsion system for transit from Earth-LEO to the L_2-Lagrange point propellant depot prior to rendezvous is calculated in Equation 58.

$$m_{e_{vehicle\,E2L2}} = \left(\frac{\epsilon}{1-\epsilon} \right) m_{P_{vehicle\,E2L2}}$$

Equation 58 – Empty mass required to support the necessary propellant mass for the Earth-to-L_2 phase of the rendezvous mission.

The gross mass value for each payload transfer vehicle configuration for the Earth-to-L_2 phase is determined using Equation 59.

$$m_{0_{vehicle\,E2L2}} = m_{P_{vehicle\,E2L2}} + m_{e_{vehicle\,E2L2}} + m_{0_{vehicle\,L2rendezvous}}$$

Equation 59 – Calculation of the gross mass quantity to support the upper/second stage-specific propulsion system for transfer from LEO to the L_2-Lagrange point propellant depot.

Table 10 – Propellant mass, empty mass, and gross mass values required a spacecraft to reach the apoapsis location of the Earth-Moon system from LEO. The gross mass values include the only the necessary empty mass values for the landing and LMO injection phases, as well as the necessary propellant and empty mass values for rendezvous at the L_2-Lagrange point propellant depot and Earth-to-L_2 stage. This is shown in Equation 59.

Staging Values from LEO to L_2-Lagrange Point Propellant Depot Prior to Rendezvous			
Propulsion System	$m_{P_{vehicle\,E2L2}}$	$m_{e_{vehicle\,E2L2}}$	$m_{0_{vehicle\,E2L2}}$
ULA – Common Centaur Upper Stage RL-10A4-2	70,492.94 kg	7,832.55 kg	139,349.28 kg
ULA – DCSS RL-10B-2	66,948.93 kg	7,438.77 kg	134,568.45 kg
SpaceX – Falcon 9 Stage 2 Merlin 1D	182,320.90 kg	20,257.88 kg	284,771.39 kg

The gross mass per phase of each mission design scenario is combined into a total

summation value to represent the global propellant mass requirement per each payload

transfer vehicle's propulsion system investigated.
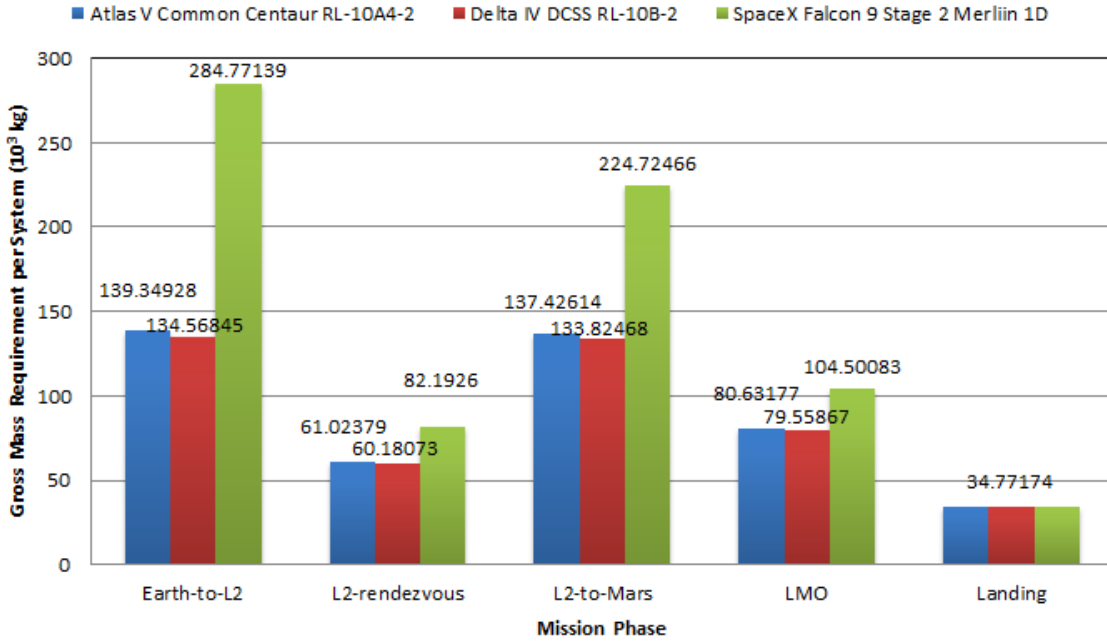
Figure 10 – Gross mass requirements per each phase within the L_2-rendezvous mission. Shown are the necessary values to support the propulsion systems for each payload transfer vehicle.

Direct Approach vs. Rendezvous Approach

The necessary Δv propulsive maneuvers for both the Mars-direct approach and L_2-rendezvous approach is illustrated in Figure 11.
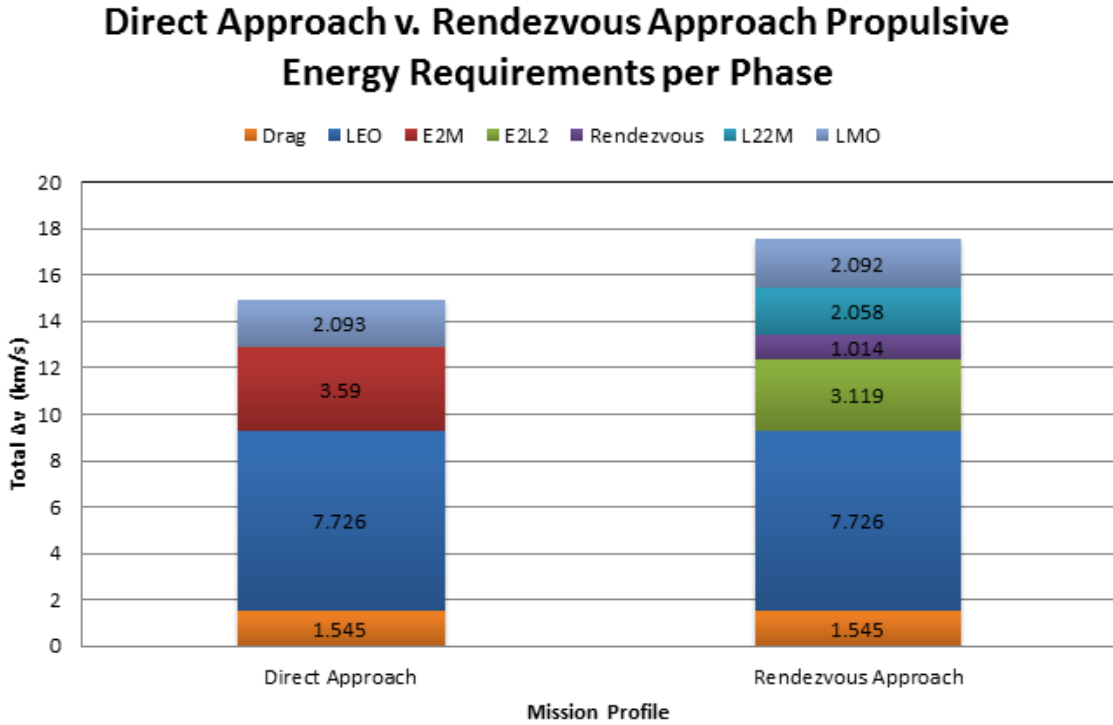
Figure 11 – Graph to illustrate the propulsive energy expenditures per each phase of the mission Values within each stacked column represent the Δv requirement (in km/s) per phase of each mission profile.

The propellant mass, empty mass, and gross mass values for the Mars-direct approach and L_2-Lagrange point propellant depot approach, separated by arrival and departure to/from rendezvous, is organized and displayed in Tables 11-13, respectively.

Table 11 – Propellant mass requirements for the Mars-direct approach and for each stage within the L_2-rendezvous approach.

Propulsion System Propellant Mass Requirements Per Mission Design Scenario						
Mission Design Scenario	ULA – Common Centaur Upper Stage RL-10A4-2		ULA – DCSS RL-10B-2		SpaceX – Falcon 9 Stage 2 Merlin 1D	
Mars-Direct Approach	156,807.53 kg		149,226.00 kg		372,992.81 kg	
L2 Rendezvous Approach	173,747.52 kg		166,068.58 kg		378,930.21 kg	
Earth-to-L2	L2-to-Mars	82,995.00 kg	90,752.52 kg	79,016.37 kg	87,052.21 kg	205,568.02 kg	173,362.19 kg

Table 12 – Empty mass requirements for the Mars-direct approach and the L_2-rendezvous approach.

Propulsion System Empty Mass Requirements Per Mission Design Scenario			
Mission Design Scenario	ULA – Common Centaur Upper Stage RL-10A4-2	ULA – DCSS RL-10B-2	SpaceX – Falcon 9 Stage 2 Merlin 1D
Mars-Direct Approach	17,372.06 kg	16,580.67 kg	41,443.65 kg
L2 Rendezvous Approach	13,574.84 kg	13,025.46 kg	29,580.98 kg

Table 13 – Gross mass requirements, including both propellant and empty mass for the Mars-direct approach and for each stage within the L_2-rendezvous approach.

Propulsion System Gross Mass Requirements Per Mission Design Scenario						
Mission Design Scenario	ULA – Common Centaur Upper Stage RL-10A4-2		ULA – DCSS RL-10B-2		SpaceX – Falcon 9 Stage 2 Merlin 1D	
Mars-Direct Approach	326,224.10 kg		317,237.07 kg		590,809.02 kg	
L2 Rendezvous Approach	453,202.72 kg		442,904.25 kg		735,961.22 kg	
Earth-to-L2	L2-to-Mars	200,373.07 kg	252,829.65 kg	194,749.18 kg	248,155.08 kg	366,963.99 kg	368,997.22 kg

The gross mass requirements, shown in Figure 12, illustrate the amount of fuel required for both mission scenarios specifically by the propulsion system for each payload transfer vehicle candidate to deliver the mission payload.
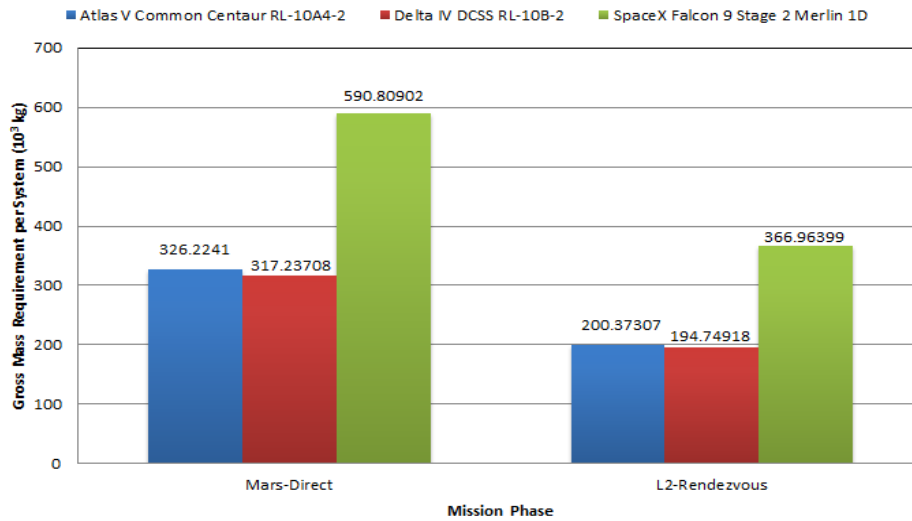
Figure 12 – Illustration to compare the gross masses required at launch from Earth for each mission scenario. The Mars-direct approach requires all fuel and empty masses to be equipped entirely within the launch vehicle for launch. The L_2-rendezvous approach requires only the necessary fuel and empty masses for the launch delivery vehicle to reach the propellant depot.

Shown in Figure 13 is an illustration breaking down and comparing the gross mass values per each mission scenario. The parameters shown include the necessary fuel and empty mass values for each specific payload transfer vehicle propulsion system.
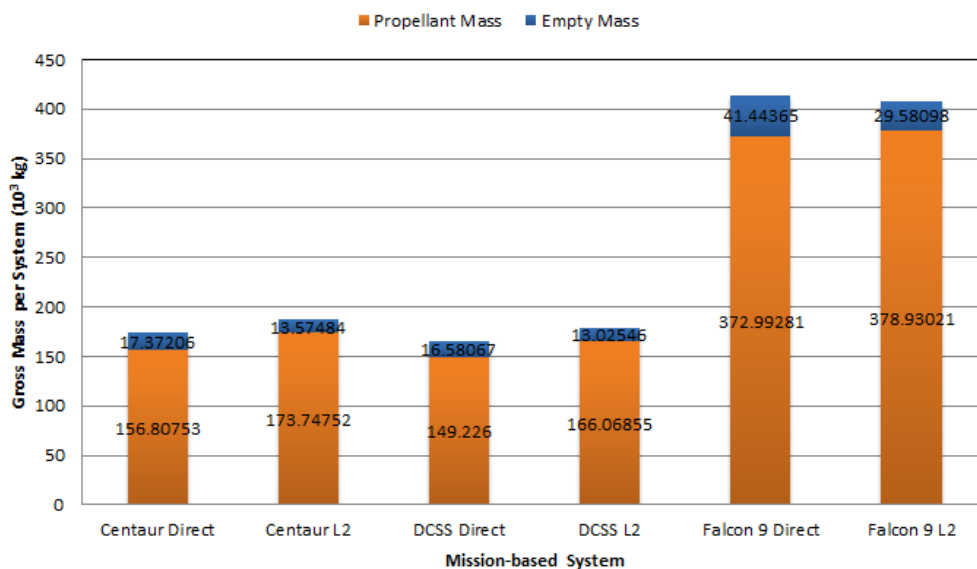
Figure 13 – Stacked allotment of propellant and empty mass quantities for each vehicle-specific propulsion system for both mission profiles.

61

Chapter IV

Discussion

Evaluations

Orbital propellant depots offer a wide range of versatility and reusability. Their prospective locations provide spacecraft an advantageous pillar for vehicle support and mission logistics. The depot provides unmanned spacecraft and crew-inhabited vehicles offer an excellent capability for supporting commercial and exploratory operations over the course of several decades [52].

Analysis conducted between the two mission design scenarios under investigation, the Mars-direct approach and the L_2-Lagrange point rendezvous approach, found significant differences in the mission requirements for both approaches. These differences are accounted for in supporting either a direct route to Mars or a rendezvous approach by way of a propellant depot located at the L_2-Lagrange point outside of the Moon. As well, differences in the necessary quantities of fuel and empty masses to sustain each of these mission designs are described in further detail.

Compared to the gross Δv value for the Mars-direct approach of $14.954 \frac{km}{s}$, the rendezvous approach requires approximately 17.4% additional propulsive energy, the difference being an additional Δv of $2.6 \frac{km}{s}$. That additional velocity is intended to fulfill rendezvous and departure propulsive energy requirements at the propellant depot.

Although there is a small additional amount of energy required by the spacecraft in order to carry out the L_2-rendezvous approach, the savings in fuel and empty mass savings at launch is substantially significant. Of the three propulsion systems investigated in this study, the Pratt & Whitney RL-10B-2 propulsion system required the lowest

propellant gross mass overall for both the direct approach and rendezvous approach.

Using this propulsion for comparing the two approaches, the propellant mass required for

the overall Mars-direct approach is 149,226.00 kilograms while the propellant mass for

the overall L_2-rendezvous approach is 166,068.58 kilograms, a differential in the added

propellant mass totaling approximately 11.3%. However, the propellant mass to be

launched from Earth for the spacecraft to reach the propellant depot for refueling is

79,016.37 kilograms. The cost savings for fueling a rocket to reach the L_2-Lagrange point

propellant depot versus a Mars-direct approach is approximately a 47.1% less amount.

The necessary empty mass to support each propulsion system under investigation

in this study was calculated for both mission profiles. Using the RL-10B-2 propulsion

system, the required empty mass for the Mars-direct approach is 16,580.67 kilograms and

13,025.46 kilograms for the L_2-rendezvous approach. Unlike the phase of the rendezvous

approach for accumulating the necessary propellant mass once the spacecraft reaches the

depot, empty mass quantities are required to be included throughout the mission in order

to support the necessary propulsion systems regardless of the phase the spacecraft is

initiating. For the purpose of this paper, the spacecraft is not being assembled with

additional vehicles in-space (i.e. LEO) or at the propellant depot. The cost savings for

designing the launch delivery vehicle and payload transfer vehicle to be equipped with

the necessary empty mass systems to support the required propellant masses is 21.4% less

for the rendezvous approach versus the Mars-direct approach.

Using the RL-10B-2 propulsion system, the gross mass required to be launched

from Earth for the Mars-direct approach is 317,237.07 kilograms while the gross mass for

the L_2-rendezvous approach is 194,749.17 kilograms. The advantage for a spacecraft to

rendezvous at the propellant depot is a 38.6% reduction in the necessary propellant mass required to be launched from Earth.

The use of conic and patched conic dynamics produced essential data to draw conclusive information for accomplishing the objectives sought in this study. Two-body approximation provided the necessary means to determining the propulsive energy requirements per phase within each approach. In fact, the use of the two-body dynamics versus the CR3BP produced data with minimal difference in the calculated result (for example, $d = v_{peri_{E2L2}} - v_j = 0.20 \, \frac{\text{km}}{\text{s}}$). Taking the injection velocity at periapsis for departure within the Earth-Moon system for the rendezvous approach and comparing it to the same burnout velocity, calculated using Equation 70 (see Appendix), which produced a differential of approximately 1.8%. This minimal error in using two-body approximations versus three-body dynamics produced insignificant differences in the data.

Calculations for rendezvous at the propellant depot were completed using a strictly Hohmann transfer. This introduced an estimated error of approximately 7% for the velocities calculated using patched conics and less than 2% in the associated mass values. While it may be suggested that data determined through the use of conic and patched conic approximations may be inaccurate for determining the actual flight paths of the Earth-Moon system, the only concern of this paper is determining the necessary impulsive maneuvers and required masses; therefore, these errors did not have an effect on the corresponding mass calculations.

Conclusions

      The analyses and procedures performed over the duration of this study provided valuable, justifiable evidence in addressing the subject of this paper, a preliminary design investigation for an interplanetary mission to Mars. These processes were constructed and performed to address the main objectives of this study: 1) determine the total Δv requirements for a rendezvous mission to a Lagrangian point propellant depot; 2) conduct a comparative analysis between a direct approach and rendezvous mission en route to Mars; 3) determine the necessary propellant requirements and any additional vehicle requirements to complete both missions.

      A comparative analysis was conducted between the control mission scenario and the secondary mission scenario for which this paper proposed. It was determined that utilizing a location for spacecraft refueling for a mission to Mars had several advantageous impacts to the mass properties of a launch delivery vehicle blasting off from Earth. First, one key advantage between the two mission profiles is the significantly lesser amount of propellant mass required to be launched to LEO en route to the propellant depot versus the substantial mass values required to be launched from Earth for the Mars-direct approach. Second, the savings in costs for missions utilizing the propellant depot outweigh the costs associated with those missions whose vehicles are loaded with the gross propellant mass at launch.

      Designing smaller vehicles capable of storing the necessary propellant masses to reach the L_2 propellant depot is far more beneficial in terms of costs than launching a large, heavy lift vehicle potentially capable of holding the gross propellant mass required for a direct mission to Mars. A reduction in launch vehicle size due to savings

implemented by rendezvous at the propellant depot increases the number of launches manifested over the year, versus using a heavy lift vehicle (i.e. SLS), which is planned to lift off only twice a year due to its significant launch costs and adequate lead time for assembly and stacking. Mapping these savings in costs over several decades will save space programs a significant amount of money in utilizing launch vehicles requiring less propellant mass to reach propellant depots for refueling versus designing and launching spacecraft to house the entire mission-profile propellant mass at launch.

It is assumed that at the time a propellant depot is placed in orbit, advances in boil-off mitigation technology and radiation shielding are present on the propellant tanks so as to prevent loss of cryogenic fuels. The 3.81% per month liquid hydrogen boil-off and 0.49% per month liquid oxygen boil-off may be mitigated by technological solutions to achieve zero boil-off (ZBO). In the case that the equipment necessary to prevent ZBO is not present on the spacecraft or the propellant depot tanks, then an increased mass of propellant will be required to counter the calculated boil-off of cryogenic fuels for both spacecraft [53].

The decision for choosing Mars as the final destination for the investigation was an example to use that is common for both mission scenarios from the point that a spacecraft departs the vicinity of Earth's SOI. This was necessary to produce a "fair" comparison of the two profiles, direct and rendezvous. This approach is a benefit to future studies because it could be used for any "common mission" for comparison of two similar mission design scenarios.

Recommendations

Completion of the two mission design approaches required the implementation of several variables during the analysis portion of this study. Determining which approach provided the greatest advantage was primarily measured by the mass savings incurred by the rendezvous approach in terms of propellant and empty mass value for the interplanetary mission to Mars. Although a final outcome was established in answer to the main objectives for which this paper was to accomplish, the multitude of variables and options available for the primary investigator to be tested and verified would have allowed for a more definitive and resounding outcome in addition to the research provided in this study.

Identifying the initial mission parameters, which included setting consistent values for the spacecraft departing Earth and arriving at Mars, was established by the primary investigator in order to analyze both mission design scenarios both on the basis of their shared constraints as well as to study their contrasting mission traits. Alteration of these limits such as parking orbit altitude about the departure and arrival bodies was hypothesized to have a potential effect on parameters such as spacecraft orbital velocity about the body and escape velocity at departure and arrival. It is believed that these changes in velocity within the spacecraft's dynamic state may have an impact on the spacecraft propellant requirements due to changes in the velocity requirements for both circularization about Earth and Mars as well as injection velocities at arrival and departure. Further analysis is suggested in order to determine the ideal parking altitude for a spacecraft to both depart Earth and arrive at Mars, whether that be by direct or rendezvous approach. Establishing an ideal orbit altitude about these planetary ideals will

provide accurate escape and injection velocities for the spacecraft, thus establishing an ideal solution for determining prime fuel expectations for the transfer(s).

Depth within the analysis, such as details regarding several of the mission phases' additional propulsive operations, would need to be considered in future analyses. These impulse maneuvers not measured within this research included rendezvous operations of the payload transfer vehicle at the L_2-Lagrange point propellant depot, attitude control propulsion for the payload transfer vehicle both during Earth circular orbit and Hohmann transfer, as well as both attitude and RCS propulsion requirements of the shroud for both Mars circular orbit. For future studies this type of analysis would need to be conducted in greater detail in order to design a spacecraft or set of payload transfer vehicles to have the capable fuel capacity to house the necessary fuel supply to complete such operation as well as determining if such a fuel supply and vehicle structure, as suggested by the main objective of this study, could be minimized both for launch and transit.

Future analysis is recommended to consider trajectorial inclinations of the transfers. Within each scenario, coplanar transfers were used per phase of each transfer. In spite of the minimal error between the inclination of the investigated bodies and the ecliptic plane, a more accurate model to determining the propulsive requirements for each mission profile would be achieved using this approach.

References

NOTE: Due to the investigation of ITAR violations occurring at NASA's Ames Research Center involving leaked military and government proprietary information, several documents and technical reports referenced within this paper were unable to be properly accredited within this section due to restricted access at the time this paper was completed. Documentation unavailable to the public, accessed prior to their quarantine, is denoted by an asterisk, '*'.

1. Amos, Jonathan. "Particles point way for NASA's Voyager." *BBC News*. June 15, 2012. October 10, 2012. < http://www.bbc.co.uk/news/science-environment-18458478>.

2. Ferris, Timothy. "Timothy Ferris on Voyagers' Never-Ending Journey." *Smithsonian Magazine*. May 2012. pp. 1-3. October 10, 2012. < http://www.smithsonianmag.com/science-nature/Timothy-Ferris-on-Voyagers-Never-Ending-Journey.html>.

3. *<http://ntrs.nasa.gov/archive/nasa/casi.ntrs.nasa.gov/20070031234_2007032394.pdf>.

4. *The NASA Authorization Act of 2010*. July 15, 2010. U.S. Senate Committee on Commerce, Science, & Transportation. September 24, 2012. <http://commerce.senate.gov/public/index.cfm?p=Legislation&ContentRecord_id=8d7c1465-f852-4835-ba84-25faf56bbb36&ContentType_id=03ab50f5-55cd-4934-a074-d6928b9dd24c&Group_id=6eaa2a03-6e69-4e43-8597-bb12f4f5aede>.

5. *What's Next for NASA?*. January 25, 2013. National Aeronautics and Space Administration. September 24, 2012. <http://www.nasa.gov/about/whats_next.html>.

6. Matthews, Mark K. "Sentinel Exclusive: NASA wants to send astronauts beyond the moon." *The Orlando Sentinel*. September 22, 2012. pp. 1-2. September 24, 2012. <http://articles.orlandosentinel.com/2012-09-22/news/os-nasa-space-outpost-20120922_1_moon-rocks-space-launch-system-nasa-chief-charlie-bolden#.UF-ZDaauoaE.email>.

7. *<http://ntrs.nasa.gov/archive/nasa/casi.ntrs.nasa.gov/20080008384_2008004081.pdf>.

8. Koon, Wang Sang; Lo, Martin W.; Marsden, Jerrold E.; Ross, Shane D. "Dynamical Systems, the Three-Body Problem and Space Mission Design." *Virginia Teach Department of Engineering Science and Mechanics*. April 25, 2011. pp. ix-x. November 1, 2012. <http://www2.esm.vt.edu/~sdross/books/KoLoMaRo_DMissionBk.pdf>.

9. *Saturn V Moon Rocket*. The Boeing Company. November 1, 2012. <http://www.boeing.com/boeing/history/boeing/saturn.page>.

10. Tate, Karl. "NASA's Mighty Saturn V Moon Rocket Explained (Infographic)." *SPACE.com*. November 9, 2012. November 2, 2012. <http://www.space.com/18422-apollo-saturn-v-moon-rocket-nasa-infographic.html>.

11. *Chapter 6: Economics and the Shuttle*. January 15, 2011. SP-4221 The Space Shuttle Decision. November 2, 2012. <http://history.nasa.gov/SP-4221/ch6.htm>.

12. Howell, Joe T.; Mankins, John C.; Fikes, John C. "In-Space Cryogenic Propellant Depot Stepping Stone." *Acta Astronautica*. 2006. pp. 230-235. October 16, 2012.

13. Nakayima, M.; Scheeres, D.J.; Yamakawa, H.; Yoshikawa, M. "Analysis of Capture Trajectories to the Vicinity of Libration Points." pp. 1. October 17, 2012.

14. Goff, Jonathan A.; Kutter, Bernard F.; Bienhoff, D.; Chandler, F.; Marchetta, J. "Realistic Near-Term Propellant Depots: Implementation of a Critical Spacefaring Capability." *American Institute of Aeronautics and Astronautics*. pp. 2. October 17, 2012.

15. *Space Shuttle Use of Propellants and Fluids*. September 2001. NASA Facts. October 20, 2012. <http://www-pao.ksc.nasa.gov/kscpao/nasafact/pdf/ssp.pdf>.

16. Pinchefsky, Carol. "5 Horrifying Facts You Didn't Know About the Space Shuttle." *Forbes Magazine*. April 18, 2012. October 20, 2012. <http://www.forbes.com/sites/carolpinchefsky/2012/04/18/5-horrifying-facts-you-didnt-know-about-the-space-shuttle/>.

17. *<http://ntrs.nasa.gov/archive/nasa/casi.ntrs.nasa.gov/20100033144_2010034555.pdf>.

18. McLean, Christopher. "Cryogenic Propellant Depots Design Concepts and Risk Reduction Activities." *University of Texas*. March 2, 2011. October 22, 2012. <http://spirit.as.utexas.edu/~fiso/telecon/McLean_3-2-11/McLean_3-2-11.pdf>.

19. Dubbink, Thomas. "Designing for Har Decher, Ideas for Martian Bases in the 20th Century." *Defelt University*. August 2001. pp. 6-14. January 30, 2013. <http://www.spacearchitect.org/pubs/dubbink/HarDecher/HarDecher.pdf>.

20. Lagrange, Joseph-Louis. "Tome 6, Chapitre II: Essai sur le probleme des trois corps".*Gallica Bibliotehque Numberique*. pp. 229-334. October 23, 2012. <http://gallica.bnf.fr/ark:/12148/bpt6k229225j/f231.image.r=Oeuvres+de+Lagrane.langFR>.

21. O'Neill, Gerard K. Wikipedia, the free encyclopedia. October 30, 2012. <http://en.wikipedia.org/wiki/Gerard_K._O%27Neill#cite_note-ONeill74-25>.

22. Michaud, Michael A.G. "Reaching for the High Frontier. The American Pro-Space Movement 1972-84." *National Space Society*. 1986. October 15, 2012. <http://www.nss.org/resources/library/spacemovement/chapter05.htm#n19>.

23. Vallado, David A. Fundamentals of Astrodaynamics and Applications. El Segundo, CA: Microcosm Press, 2001; Norwell, MA: Kluwer Academic Publishers, 2001.

24. Curtis, Howard D. Orbital Mechanics for Engineering Students. Burlington, MA: Elsevier Ltd., 2010.

25. Lutze, Frederick H. "Summary of Patched Conic Approximation." *Virginia Tech Aerospace and Ocean Engineering*. November 2, 2012. <http://www.dept.aoe.vt.edu/~lutze/AOE4134/patchedconiceqs.pdf>.

26. *Lagrange Points of the Earth-Moon System*. March 2, 2012. Mechanics. October 30, 2012. <http://hyperphysics.phy-astr.gsu.edu/hbase/mechanics/lagpt.html>.

27. Tokoro, Shinichi. "The Restricted Three-Body Problems." *College of the Redwoods*. 2007. March 15, 2013. <http://online.redwoods.edu/instruct/darnold/DEProj/sp02/shinichi/ODESlideshow.pdf>.

28. Fitzpatrick, Richard. "Stability of Lagrange Points." *Institute for Fusion Studies, University of Texas*. March 31, 2011. April 21, 2013. <http://farside.ph.utexas.edu/teaching/336k/Newtonhtml/node126.html>.

29. *<http://ntrs.nasa.gov/archive/nasa/casi.ntrs.nasa.gov/20100027329_2010028976.pdf>.

30. *Mars Exploration Program*. National Aeronautics and Space Administration: Jet Propulsion Laboratory. October 15, 2012. <http://mars.jpl.nasa.gov/programmissions/missions/log/>.

31. *<ntrs.nasa.gov/archive/nasa/casi.ntrs.nasa.gov/20100028285_2010030306.pdf>.

32. *The Case for Mars: Concept Development for a Mars Research Station*. National Aeronautics and Space Administration: Jet Propulsion Laboratory. April 15, 1986. November 2, 2012. <https://dl-web.dropbox.com/get/Thesis/The%20Case%20for%20Mars__Concept%20Development%20for%20a%20Mars%20Research%20Station.pdf?w=AAC7kRa8lEljei8JstPQpBen_ftrU8fVfidguKZzyYFhEA>.

33. Dorsey, John T.; Wu, K. Chauncey; Smith, Russ. "Structural Definitions and Mass Estimation of Lunar Surface Habitats for the Lunar Architecture Team Phase 2 (LAT-2) Study." *NASA Langley Research Center*. December 5, 2012.

34. *Mars Exploration. A Tour of Past, Present, and Future Exploration*. National Aeronautics and Space Administration: Goddard Space Flight Center. January 6, 2005. March 24, 2013. <http://nssdc.gsfc.nasa.gov/planetary/mars/image/bigland.gif>.

35. *<ntrs.nasa.gov/archive/nasa/casi.ntrs.nasa.gov/20100028285_2010030306.pdf>.

36. *Mars Society Mission*. Encyclopedia Astronautica. December 5, 2012. <http://www.astronautix.com/craft/marssion.htm>.

37. *Standard Gravitational Parameter*. Wikipedia, the free encyclopedia. November 2, 2012. <http://en.wikipedia.org/wiki/Standard_gravitational_parameter>.

38. Doody, Dave. "Basics of Space Flight Section I: Chapter 4. Interplanetary Trajectories." *Jet Propulsion Laboratory California Institute of Technology*. Fisher, Diane. April 23, 2003. <http://www2.jpl.nasa.gov/basics/bsf4-1.php>.

39. *<http://ntrs.nasa.gov/archive/nasa/casi.ntrs.nasa.gov/20100028911_2010028560.pdf>.

40. *Atlas V Launch Services User's Guide*. March 2010. United Launch Alliance. January 15, 2013. <http://www.ulalaunch.com/site/docs/product_cards/guides/AtlasVUsersGuide2010.pdf>.

41. *Evolved Expendable Launch Vehicle*. November 2, 2011. Air Force Space Command. January 15, 2013. <http://www.afspc.af.mil/library/factsheets/factsheet.asp?id=3643>.

42. *Delta IV Payload Planners Guide*. September 2007. United Launch Alliance. January 15, 2013. <http://www.ulalaunch.com/site/docs/product_cards/guides/DeltaIVPayloadPlannersGuide2007.pdf>.

43. Chang, Kenneth. "SpaceX Capsule Docks at Space Station." *The New York Times*. May 25, 2012. October 11, 2012. <http://www.nytimes.com/2012/05/26/science/space/space-x-capsule-docks-at-space-station.html?_r=1&>.

44. McGarry, Brendan. "SpaceX Becomes First Company to Dock Ship at Space Station." *Bloomberg*. May 25, 2012. October 11, 2012. <http://www.bloomberg.com/news/2012-05-25/spacex-becomes-first-company-to-dock-ship-at-space-station-1-.html>.

45. "SpaceX Plans to be World's Top Rocket Maker." *Aviation Week and Space* Technology. August 8, 2011. October 11, 2012. <http://www.aviationweek.com/publication/awst/loggedin/AvnowStoryDisplay.do?fromChannel=awst&pubKey=awst&channel=awst&issueDate=2011-08-08&story=xml/awst_xml/2011/08/08/AW_08_08_2011_p27-354586.xml&headline=SpaceX+Unveils+Plans+To+Be+World%26rsquo%3Bs+Top+Rocket+Maker>.

46. Bergin, Chris. "SLS J-2X Upper Stage Engine Enjoys Successful 500 Second Test Fire." *NASASpaceflight.com*. Dr. Nox & Associates. November 9, 2011. January 15, 2013. <http://www.nasaspaceflight.com/2011/11/sls-j-2x-upper-stage-engine-500-second-test-fire/>.

47. *<http://ntrs.nasa.gov/archive/nasa/casi.ntrs.nasa.gov/20100017668_2010017622.pdf>.

48. Kyle, Ed. "NASA's Space Launch System." *Space Launch Repot – Space Launch System Data Sheet*. January 22, 2013. February 2, 2013. <http://www.spacelaunchreport.com/sls0.html>.

49. *<http://ntrs.nasa.gov/archive/nasa/casi.ntrs.nasa.gov/20100017229_2010017720.pdf>.

50. Braun, Robert D.; Manning, Robert M. "Mars Exploration Entry, Descent, and Landing Challenges." *NASA Jet Propulsion Laboratory*. pp. 25-28. April 20, 2013. <http://trs-new.jpl.nasa.gov/dspace/bitstream/2014/39664/1/05-3869.pdf>.

51. *Aerobraking*. March 18, 2013. Wikipedia, the free encyclopedia. March 15, 2013. <http://en.wikipedia.org/wiki/Aerobraking>.

52. Smitherman, David.; Woodcock, Gary. "Space Transportation Infrastructure Supported by Propellant Depots." *American Institute of Aeronautics and Astronautics*. March 15, 2013. <http://www.nss.org/articles/Space_Transportation_Infrastructure_Supported_by_Propellant_Depots.pdf>.

53. *Drawbacks of Cryogenic Propellants*. March 20, 2013. Space Travel Guide. April 23, 2013. <http://library.thinkquest.org/03oct/02144/text/propulsion/propellents/crydraw.htm>.

54. Cornish, Neil J.; Goodman, Jeremy. "The Lagrange Points." *Montana State University*. March 20, 2013. <http://www.physics.montana.edu/faculty/cornish/lagrange.pdf>.

Appendix

Derivation of the Equations of Motion for the CR3BP

The spacecraft is located within a sidereal system (coordinate system rotating about the barycenter of the two bodies), referenced by a set of rotating, non-dimensional barycentric equations of motions (Equation 60) [27] which determine the accelerations in the respective degree of motion based on the difference between the sidereal coordinate system of the spacecraft (a_{body},b_{body},c_{body}) and the sidereal coordinate system of the two-bodies (a,b,c).

$$\ddot{a} = u_1 \left(\frac{a_1 - a}{r_1^3} \right) + u_2 \left(\frac{a_2 - a}{r_2^3} \right)$$

$$\ddot{b} = u_1 \left(\frac{b_1 - b}{r_1^3} \right) + u_2 \left(\frac{b_2 - b}{r_2^3} \right)$$

$$\ddot{c} = u_1 \left(\frac{c_1 - c}{r_1^3} \right) + u_2 \left(\frac{c_2 - c}{r_2^3} \right)$$

Equation 60 – Equations of motion of the particle in the sidereal system [27].

The radial distances of the two bodies relative to within the two-body system are represented in Equation 61.

$$r_1^2 = (a_1 - a)^2 + (b_1 - b)^2 + (c_1 - c)^2$$

$$r_2^2 = (a_2 - a)^2 + (b_2 - b)^2 + (c_2 - c)^2$$

Equation 61 – Length parameters from the primary bodies to the spacecraft.

Converting Equations 61 produced the results shown in Equations 62, where (x,y,z) represent the coordinates of the spacecraft with respect to synodic (rotating) system.

$$r_1^2 = (x + u_2)^2 + y^2 + z^2$$

$$r_2^2 = (x - u_1)^2 + y^2 + z^2$$

Equation 62 – Conversion from Equation 61 using the location of the spacecraft in three-dimensional space.

To obtain the equations of acceleration, the second derivative of Equation 63 is taken and

presented in Equation 64.

$$\begin{bmatrix} a \\ b \\ c \end{bmatrix} = \begin{bmatrix} \cos \Omega t & -\sin \Omega t & 0 \\ \sin \Omega t & \cos \Omega t & 0 \\ 0 & 0 & 1 \end{bmatrix} \begin{bmatrix} x \\ y \\ z \end{bmatrix}$$

Equation 63 – Relationship between the coordinates of the spacecraft by its rotation within the system. The symbol Ω represents the inertial angular velocity [27].

$$\begin{bmatrix} \ddot{a} \\ \ddot{b} \\ \ddot{c} \end{bmatrix} = \begin{bmatrix} \cos \Omega t & -\sin \Omega t & 0 \\ \sin \Omega t & \cos \Omega t & 0 \\ 0 & 0 & 1 \end{bmatrix} \begin{bmatrix} \ddot{x} - 2\Omega \dot{y} - \Omega^2 x \\ \ddot{y} + 2\Omega \dot{x} - \Omega^2 y \\ \ddot{z} \end{bmatrix}$$

Equation 64 – Second-order differential of Equation 63 [27].

Replacing the values of a, b, c, $\ddot{a}$, $\ddot{b}$, $\ddot{c}$, the Corioli and centrifugal acceleration, is conducted in

Equation 65.

$$\left(\ddot{x} - 2\Omega \dot{y} - \Omega^2 x \right) \cos \Omega t - \left(\ddot{y} + 2\Omega \dot{x} - \Omega^2 y \right) = \left[u_1 \left(\frac{x_1 - x}{r_1^3 + u_2} \frac{x_2 - x}{r_2^3} \right) \right] \cos \Omega t + \left[\frac{u_1}{r_1^3} + u_2 r_2^3 \right] y \sin \Omega t$$

$$\left(\ddot{x} - 2n\dot{y} - \Omega^2 x \right) \sin \Omega t - \left(\ddot{y} + 2n\dot{x} - \Omega^2 y \right) = \left[u_1 \left(\frac{x_1 - x}{r_1^3 + u_2} \frac{x_2 - x}{r_2^3} \right) \right] \cos \Omega t + \left[\frac{u_1}{r_1^3} + u_2 r_2^3 \right] y \cos \Omega t$$

$$\ddot{z} = - \left[\frac{u_1}{r_1^3} + \frac{u_2}{r_2^3} \right] z$$

Equation 65 – Matrix multiplication of Equation 64 [27].

Derivation of the Jacobi Integral

Using the scalar function U, Equation 67 is written as the gradient of the accelerations

where $U = U(x, y, z)$ is given by Equation 66.

$$U = \frac{\Omega^2}{2} (x^2 + y^2) + \frac{\mu_1}{r_1} + \frac{\mu_2}{r_2}$$

Equation 66 – Scalar function representation for simplification the acceleration equations [27].

$$\ddot{x} - 2\Omega\dot{y} = \frac{\partial U}{\partial x}$$

$$\ddot{y} - 2\Omega\dot{x} = \frac{\partial U}{\partial y}$$

$$\ddot{z} = \frac{\partial U}{\partial z}$$

Equation 67 – Scalar equations for the CR3BP [27].

Multiplying each function within Equation 67 by $\dot{x}$, $\dot{y}$, and $\dot{z}$, respectively, and combined produces Equation 68.

$$\dot{x}\ddot{x} + \dot{y}\ddot{y} + \dot{z}\ddot{z} = \frac{\partial U}{\partial x}\dot{x} + \frac{\partial U}{\partial y}\dot{y} + \frac{\partial U}{\partial z}\dot{z} = \frac{\partial U}{\partial t}$$

Equation 68 – Finding the Jacobi integral through the use of the spacecraft's position and velocity [27].

Integration of Equation 68 produces Equation 69, where C_j is the constant of integration.

$$\dot{x}^2 + \dot{y}^2 + \dot{z}^2 = 2U - C_j$$

Equation 69 – Integrated solution of Equation 68 [27].

The magnitude of the velocity of the spacecraft in three-dimensional space is known as $v_j^2 = \dot{x}^2 + \dot{y}^2 + \dot{z}^2$, where taking the square of this function produced Equation 70 to find Jacobi's constant.

$$C_j = \Omega^2(x^2 + y^2) + 2\left(\frac{\mu_1}{r_1} + \frac{\mu_2}{r_2}\right) - v_j^2$$

Equation 70 – Calculation to determine Jacobi's Constant, used to analyze the location of the spacecraft where its velocity is denoted as zero, providing boundary curves that the spacecraft cannot penetrate. A Jacobi constant value of $10.865 \frac{\text{km}}{\text{s}}$ was used to compare the patched conic approximations conducted in the paper with the CR3BP [24, 27].

Determination of the Lagrange Points

Setting $y = 0$, the three collinear Lagrange points L_1, L_2, and L_3 are found by solving for x in Equation 70. The locations in a two-dimensional frame are found in Equation 71, where $= 1 \text{ AU} \approx 1.5 \times 10^8 \text{ km}$ [54].

$$L_1: \left(R\left[1 - \left(\frac{\frac{m_2}{m_1+m_2}}{3}\right)^{\frac{1}{3}}\right], 0\right)$$

$$L_2: \left(R\left[1 + \left(\frac{\frac{m_2}{m_1+m_2}}{3}\right)^{\frac{1}{3}}\right], 0\right)$$

$$L_3: \left(-R\left[1 + \frac{5}{12}\frac{m_2}{m_1+m_2}\right], 0\right)$$

Equation 71 – Determination of the coordinates for the L_1, L_2, and L_3 Lagrange points in a two-body system.

Finding the two triangular equilibrium points, L_4 and L_5, is done by designating $r_1 = r_2 = 1$ [54]. These Lagrange point coordinates, mirror reflections of one another sitting at opposite points of each equilateral triangle vertex, is shown in Equation 72.

$$L_4: \left(\frac{R}{2}\left(\frac{m_1-m_2}{m_1+m_2}\right), \frac{\sqrt{3}}{2}R\right)$$

$$L_5: \left(\frac{R}{2}\left(\frac{m_1+m_2}{m_1+m_2}\right), -\frac{\sqrt{3}}{2}R\right)$$

Equation 72 – Determination of the coordinates for the L_4 and L_5 Lagrange points in a two-body system.

Methodology for Calculating the Mass Requirements

The process to determine the propellant, empty, and gross mass values required to execute each mission design phase per approach is shown.

$$m_{P_{phase}} = m_{f_{phase}}\left(e^{\frac{\Delta v_{phase}}{Isp_{vehicle}g_0}} - 1\right)$$

$$m_{P_{phase}} = m_{f_{phase}}\left(e^{\frac{\Delta v_{phase}}{c_{vehicle}}} - 1\right)$$

Equation 73 – To calculate the propellant mass requirements based on a specific impulse parameter for the chosen payload transfer vehicle's propulsion system along with the required velocity requirement previously determined per each phase for each mission design approach [24].

The final launch vehicle mass refers to the mass of the rocket following burnout at during the phase in question. This includes the empty mass of the vehicle including the engines, fuel tanks, control systems, etc., as well as the mission payload mass. A structural ratio value is the vehicle empty mass relative to the vehicle gross mass excluding the mission payload.

$$\epsilon = \frac{m_{e\,phase}}{m_{e\,phase} + m_{P\,phase}}$$

Equation 74 – To calculate the structural ratio value based on the empty vehicle mass to total vehicle mass (excluding mission payload mass) ratio [24].

Solving for the empty mass structure, the vehicle mass following burnout, Equation 74 is simplified into Equation 75.

$$m_{e\,phase} = \left(\frac{\epsilon}{1-\epsilon}\right) m_{P\,phase}$$

Equation 75 – To calculate the empty vehicle mass based on Equation 74.

The vehicle gross is the summation of the propellant mass requirement, empty mass, and payload mass to be delivered, shown in Equation 76. When combined with the mass ratio rocket equation in Equation 77, the propellant mass calculation is simplified in Equation 78.

$$m_{0\,phase} = m_{e\,phase} + m_{P\,phase} + m_{P/L}$$

Equation 76 – To calculate the required gross propellant mass per phase for each mission design approach.

$$\frac{m_{0\,phase}}{m_{f\,phase}} = e^{\frac{\Delta v_{phase}}{c_{vehicle}}}$$

Equation 77 – Mass ratio rocket equation, calculating the ratio of gross vehicle mass to final vehicle mass following burnout [24].

$$m_{P\,phase} = \left[m_{P/L} + \frac{\epsilon}{1-\epsilon} m_{P\,phase}\right] e^{\frac{\Delta v_{phase}}{c_{vehicle}}} - \frac{\epsilon}{1-\epsilon} m_{P\,phase} - m_{P/L}$$

Equation 78 – Simplified arrangement of Equation 76 and Equation 77.

Combining terms in solving for propellant mass requirement s per each phase is assembled in Equation 79.

$$m_{P_{phase}} = m_{P/L} \left(\frac{(1-\epsilon)\left(e^{\frac{\Delta v_{phase}}{c_{vehicle}}} - 1 \right)}{\left(1 - \epsilon e^{\frac{\Delta v_{phase}}{c_{vehicle}}} \right)} \right)$$

Equation 79 – Final simplified equation to calculate the vehicle propellant mass requirements per phase.